

University of Southern Queensland
Faculty of Engineering and Surveying

Analysis of the behaviour of composite transom decks for railway Bridges

A dissertation submitted by:
Mr Scott Walker

Supervised by
Dr Allan Manalo

In fulfilment of the requirements of
Engineering research project

ABSTRACT

Hardwood has been the preferred material for railway sleepers and maintenance work on existing timber sleeper track continues to be provided by hardwoods. Worldwide, there are more than 35 million timber sleepers required to maintain the track quality into a specified level of service. In Australia alone, railway lines require in excess of 2.5 million timber sleepers per year for railway maintenance. Over the past decade, it has been increasingly difficult to get good quality and large section of hardwood timber in quantities to keep up with demand especially in maintaining existing timber-sleeper railway lines. This trend is set to continue and will become critical within the foreseeable future, hence there is an urgent need to develop a sleeper product made from renewable resources.

Research and development has now focused on composite materials as the key performance characteristics of timber sleepers can be simulated using this material. Railway sleepers from composite materials showed the highest potential among the alternative sleeper materials for replacement of timber sleepers in the existing railway lines including transoms. Transoms are large sleepers used on railway bridges to transfer the loads from the rails to the bridge girders. In general there is no ballast present and the transoms have to transfer all the loads. The loads on the transoms depend on the position of the rails relative to the bridge beams. In Australia, the rails and the support beams are generally off-set which creates significant bending moments and shear forces in the transom. Thus, careful consideration is needed to account for the off-set of the rails in the design of the railway transom.

This project will investigate the potential use and analyse the suitability of composite sandwich structures in the development of transom decks for use on railway bridges. Finite element modelling and simulation using strand7 finite element software will be implemented to investigate the overall performance of the composite sandwich transom decks under the wheel loading due to the passing train. Conclusions on the suitability composite sandwich structures for use as transom decking is drawn, orientations and laminations determined as well as recommendations for future research suggested.

**University of Southern Queensland
Faculty of Health, Engineering and Sciences
ENG4111/ENG4112 Research Project**

Limitations of Use

The Council of the University of Southern Queensland, its Faculty of Health, Engineering & Sciences, and the staff of the University of Southern Queensland, do not accept any responsibility for the truth, accuracy or completeness of material contained within or associated with this dissertation. Persons using all or any part of this material do so at their own risk, and not at the risk of the Council of the University of Southern Queensland, its Faculty of Health, Engineering & Sciences or the staff of the University of Southern Queensland.

This dissertation reports an educational exercise and has no purpose or validity beyond this exercise. The sole purpose of the course pair entitled "Research Project" is to contribute to the overall education within the student's chosen degree program. This document, the associated hardware, software, drawings, and other material set out in the associated appendices should not be used for any other purpose: if they are so used, it is entirely at the risk of the user.

Disclaimer

I certify that the ideas, experimental work, results, analyses, software and conclusions reported in this dissertation are entirely my own effort, except where otherwise acknowledged. I also certify that the work is original and has not been previously submitted for any other award, except where otherwise acknowledged.

Acknowledgements

I would like to thank my supervisor Dr Allan Manalo for his guidance throughout the course of my project. I would also like to thank my wife for reminding me to eat during the writing of my dissertation and providing support and encouragement throughout the whole process.

ABSTRACT	iii
Notations	xi
Chapter 1 - Introduction	1
1. Introduction	1
1.1. Introduction	1
1.2. The Problem	3
1.3. Research Objectives	4
1.4. Conclusions	4
Chapter 2 - Literature Review	6
2. Review of literature on decking/sleeper Material	6
2.1. General	6
2.2. Timber	6
2.2.1. Hardwood	8
2.2.2. Softwood	8
2.2.3. Plywood	8
2.3. Concrete	8
2.4. Steel	9
2.5. Need for new type of sleeper	9
2.6. Composite sandwich structure	9
2.6.1. Properties	10
2.6.2. Applications	10
2.7. Conclusions	10
Chapter 3 - Methodology	11
3. Methodology	11
3.1. Track design	11
3.1.1. Rail curvature	11
3.1.2. Gauge	11
3.1.3. Cross Ties	11
3.2. Track Loads	11
3.2.1. 300LA track Load	11
3.3. Bending Moment and Shear	14
3.3.1. Bending Moment	14
3.3.2. Shear	14
3.3.3. Conclusion	14
Chapter 4 - Bridge Transoms	16
4. Fibre Composite transom dimensions	16
4.1. Single Sandwich	17
4.1.1. Introduction	17
4.1.2. Design for Bending	18
4.1.3. Design for shear	21
4.1.4. Flatwise Results	22
4.2. Edge single sandwich	22
4.2.1. Design for bending	22
4.2.2. Design for Shear	23
4.2.3. Edgewise Results	24
4.3. Multiple Flatwise Sandwich	24
4.3.1. Multiple Flatwise Sandwich Design for Bending	25
4.3.2. Multiple Flatwise Sandwich Design for Shear	27

4.3.3.	Multiple Flatwise Sandwich Conclusion	27
4.4.	Multiple Edge Sandwich Design for Bending	29
4.4.1.	Multiple Sandwich Edge Layout Design for Shear	30
4.4.2.	Multiple Sandwich Edge Layout Conclusion	30
4.5.	Combination Layout	30
4.5.1.	Combination design for bending	31
4.5.2.	Combination design for shear	31
4.5.3.	Combination design conclusion	32
4.6.	Conclusions	33
Chapter 5 - Transom Panel		34
5.	Rail Loads for Bridge Deck Panel	34
5.1.	Analysis in bending/Shear	35
5.1.1.	Multiple Flat Sandwiches	35
5.1.2.	Multiple Edge Sandwiches	36
5.1.3.	Multiple Combination Panel	36
5.2.	Analysis in Shear	37
5.3.	Conclusions	37
Chapter 6 - Finite Element Analysis		38
6.	Finite Element Analysis	38
6.1.	Finite Element Models	38
6.2.	Modelling Results	41
6.2.1.	Transom Beams 290 w x 209 h	41
6.2.2.	Panels 1200 w x 209 h	44
Chapter 7 - Conclusions		47
7.	Conclusions	47
7.1.	Summary	47
7.2.	Major Conclusions	47
7.3.	Application to railway transom decking	47
7.4.	Future recommended research	48
References		49
Appendices		52
A.	Flexural Stiffness flatwise and edgewise	52

Figure 1: Open Deck Bridge (Yong, 2009)	1
Figure 2: Ballast Deck (Crouch Engineering, 2014)	1
Figure 3: Rail Offset Example	2
Figure 4: Example Transom Decking	3
Figure 5: Failure due to fungal attack (Ferdous & Manalo 2014)	7
Figure 6: End Split (Ferdous & Manalo 2014)	7
Figure 7: Termite affected wood	7
Figure 8: 300LA load system (AS 5100).....	12
Figure 9: Bending Moment Diagram.....	15
Figure 10: Shear Force Diagram.....	15
Figure 11: Panel Layout and Orientations	16
Figure 12: Positive Bending.....	17
Figure 13: Flat Sandwich Moduli.....	19
Figure 14: Edgewise layout	22
Figure 15: Combination Layout.....	30
Figure 16: Proposed Panel Layout	34
Figure 17: F.E. Model for specimen BS1F	39
Figure 18: F.E. Model for Specimen BM4F.....	39
Figure 19: F.E. Model for Specimen BM4E.....	39
Figure 20: F.E. Model for Specimen BM4C	40
Figure 21: F.E. Model for Specimen PM10F.....	40
Figure 22: F.E. Model for Specimen PM10E.....	40
Figure 23: F.E. Model for specimen PM10C.....	41
Figure 24: F.E. Model BS1F Shear	41
Figure 25: F.E. Model BS1F Stress.....	41
Figure 26: F.E. Model BM4F Shear	42
Figure 27: F.E.M. BM4F Axial Stress.....	42
Figure 28: F.E. Model BM4E Shear	42
Figure 29: F.E. Model BM4E Axial Stress.....	43
Figure 30: F.E. Model BM4C Shear	43
Figure 31: F.E. Model BM4C Axial Stress	43
Figure 32: F.E. Model PM10F Shear	44
Figure 33: F.E. Model PM10F Axial Stress.....	44
Figure 34: F.E. Model PM10E Shear.....	45
Figure 35: F.E. Model PM10E Axial Stress.....	45
Figure 36: F.E. Model PM10C Shear.....	46
Figure 37: F.E. Model PM10C Axial Stress	46

Table 1: Values of Alpha (AS5100)	13
Table 2: Transom Spacing (Railcorp 2015).....	13
Table 3: Load Factors (AS5100).....	14
Table 4: Properties of Core and Skin of Sandwich	17
Table 5: Single Sandwich Flatwise.....	22
Table 6: Single Sandwich Edgewise.....	24
Table 7: Multiple Flatwise Layout	26
Table 8: 300mm High Multiple Flat Sandwich	27
Table 9: 350 mm Wide Multiple Flat Sandwich	28
Table 10: Multiple Edgewise layout	29
Table 11: Combination Layout part 1	32
Table 12: Multiple Flatwise Layout Panel	35
Table 13: Edgewise Multiple Sandwich Layout panel.....	36
Table 14: Combination Layout Panel	36
Table 15: F.E. model for Sandwich Beam.....	38

Notations

<i>Notation</i>	<i>Description</i>
b	Width of the beam (mm)
C	Thickness of the Core (mm)
d	Distance between skin centroids (mm)
D	Thickness of the overall sandwich (mm)
E_c	Young's Modulus of the Core
EI	Flexural Stiffness
E_s	Young's Modulus of the Skin
I	Moment of inertia of the cross-section mm^4
M	Bending moment at a given cross section N.mm
N_g	Ratio of shear modulus (Skin to core)
P_c	Ultimate Shear Force
P_E	Shear force edge orientation
P_F	Shear Force flat orientation
Y	Distance from the neutral plane to a particular fibre, in mm
σ	Bending stress in Mpa
σ_c	Stress in the Core
σ_s	Stress in the Skin
τ_c	Shear force in the Core (kN)
τ_s	Shear force in the Skin (kN)

Chapter 1 - Introduction

1. Introduction

“Not too long ago the problems of cross ties were solely in terms of the wood tie” (Hay 1982)

1.1. Introduction

Railroad bridges are predominantly simple-span structures (Duan 1999). This simple-span structure has a deck which provides the support structure for the rails supported by girders and usually a trestle type footing. Rail bridge decks are usually one of two different designs those being open deck (Figure 1), or ballast deck (Figure 2).



Figure 1: Open Deck Bridge (Yong, 2009)



Figure 2: Ballast Deck (Crouch Engineering, 2014)

Open deck bridge designs have the cross ties directly supported by the bridge girders. Due to the much lower dead loads of open deck bridge design, they are the most common form of railway bridge deck. Open deck rail bridges, however, transfer more of the dynamic load from the rail live load into the supporting structure than ballast decks (Duan 1999).

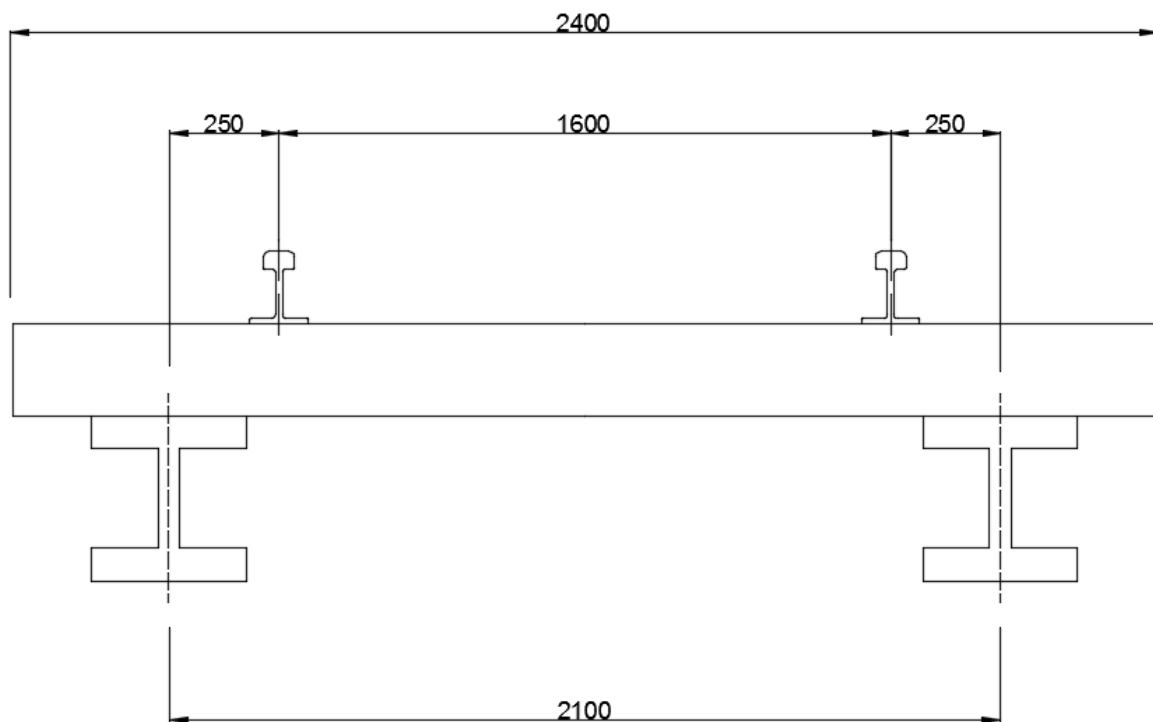


Figure 3: Rail Offset Example

In the design of open deck bridges, the rail is often at an offset to the bridge girders. This is done so that any re-alignment of the rail may be performed without the need to move the girders (Esveld 2001). Wider girders also allow for better stability (in relation to wind loading) of the bridge and offsetting the rails allows the girders to be positioned wider than the gauge and thus better handle wind loads (Duan 1999). The effect of having the rails offset to the support girders is that it creates both a bending moment and shear in the cross ties. The bending moment and shear requires bridge cross ties to be of greater dimensions than those of standard railway sleepers as standard sleepers are fully supported along their length and are not required to carry these types of loads. The bridge cross ties are still placed at similar spacing to standard railway sleepers, namely 600 mm centres and the rail offset has a maximum limit of 250mm, but usually much less (Hay 1982).

This report concentrates on another less-common type of open bridge deck called transom decking Figure 4. Transom decking differs to cross ties by the simple fact that it presents as that of a uniform level surface similar to that of a walking bridge. For a bridge with transom decking, the rails are directly fixed to this uniform gapless surface and the panels. The decking perform the role of cross ties, that of keeping the rails at the set gauge, and transferring the rail loads to the substructure of the bridge (Hay 1982). Rails are directly fixed at the same spacing of 600mm, usually by clamp plates bolted through the decking.

The major advantage of this kind of bridge decking is safety. During construction and maintenance the bridge presents with a uniform surface safe for walking on which eliminates the risk of falling through or tripping. Other advantages of transom decking over the normal cross ties are:

- The transom deck provides a barrier for both the supporting structure beneath the deck and anything else below on the ground from objects falling off the passing train.
- The decking also protects the supporting structure of the bridge from sun and moisture.
- The transom decking also provides a suitable walking surface for pedestrian crossing if required.



Figure 4: Example Transom Decking

1.2. The Problem

Existing bridge cross ties are made predominantly from hardwood. Existing wooden cross ties have the desirable material property combination of flexibility and workability not found in other materials (Hibbeler, 2004). The drawback of hard wood is that it has a limited life span of approximately 20 years if chemical treatment (Profillidis 1995). Without treatment, the life expectancy can be greatly reduced by natural factors, which in Queensland, is predominantly fungal decay (Hagaman 1992), but also includes insect attack. At the end of the cross-tie life cycle the transom must be replaced which is where this project is positioned.

Hard wood of suitable size for rail sleepers is becoming rarer and more expensive as the amount of hardwood available for production is reduced due to both government regulation and environmental pressure (Mcleod 1991). Due to Rail Bridge cross ties being nearly 100% larger than normal cross ties, sources of larger hardwood trees must be secured which increases the cost further. Annually, the rail industry spends over 35% of its annual budget on maintenance of sleepers (Yun 2003), with bridge transoms accounting for a significant percentage of that.

This has opened the door for development of alternative and renewable materials, previously considered too expensive. Currently, rail bridge decking is constructed from plywood developed specifically for the purpose and as a direct replacement for current bridge cross-ties (B4B, 2011). Plywood consists of glued laminations of thin wood veneers at 90 degree orientations. Plywood presents a viable option as bridge decking, but suffers from the similar problems to hardwood in that it is a natural product that suffers from natural degradation.

This project seeks to determine the suitability of a particular fibre composite sandwich material to act as bridge transom decking.

This project will undertake the following:

- Research the existing materials used for rail bridge decks including material strength characteristics and material orientation.
- Identify the advantages and disadvantages of existing materials specifically looking at the Australian rail bridge scenario.
- Identify the different parameters that affect the behaviour of transoms, including loading cases, railway geometry, and type of transom.
- Analyse the effects of different design parameters on the overall behaviour of transom decks using the Strand 7 finite element simulation software.
- Investigate the suitability of a proposed structural composite sandwich for transom decks through finite element simulation and analysis.
- Investigation of the best arrangement for the sandwich panels in the transom deck that will result in optimal structural performance.

1.3. Research Objectives

The aim of this study is to investigate the behaviour of a fibre composite sandwich structure and determine its potential application for replacement of railway timber decking.

The main objectives of the study are the following:

- Characterise the mechanical behaviour of existing bridge decking
- Evaluate the mechanical behaviour of an individual fibre composite sandwich structure in the flatwise and in the edgewise positions, theoretically, and by finite element modelling
- Investigate the flexural and shear behaviour of the composite sandwich structures numerically and via finite element modelling
- Determine the suitability of the fibre composite sandwich for rail bridge decking

1.4. Conclusions

This thesis is divided into chapters which cover the research objectives in a structured way.

Chapter 1 is an introduction and outlines the objectives of this study.

Chapter 2 provides a literature review on existing materials for railway transom decking, dealing with the following:

- Suitability to rail decking using Australian construction techniques
- The materials consequent issues for use as a railway bridge decking.
- The practicality of composite sandwich structures becoming a suitable alternative for railway bridge decking

Chapter 3 conducts an investigation on the behaviour of bridge cross-ties in a normal railway bridge, including investigation of rail loads to define the requirements for the alternative fibre composite sleepers.

Chapter 4 is concerned with the investigation of the mechanical properties of the fibre composite sandwich panel for its effective use as a replacement for individual bridge cross ties in both flatwise and edgewise positions for single and multiple sandwich laminations.

Chapter 1 - Introduction

Chapter 5 investigates the flexural and shear behaviour of the composite sandwich structure as a decking panel via numerical investigations.

Chapter 6 presents the finite element modelling for beams and panels

Chapter 7 present the conclusions found in the research and recommendations for future work.

Chapter 2 - Literature Review

2. Review of literature on decking/sleeper Material

2.1. General

This chapter provides general information about the properties of current railway bridge cross ties and transom decks for railway bridges including the potential use as deck panelling.

2.2. Timber

Timber has been the main stay of railway sleepers since the inception of rail. In Australia the replacement of wooden rail components accounts for over 280 000 m³ of timber (Griffin et al. 2014). Timber has the desirable natural properties of flexibility and workability. The workability allows sleepers to be repaired, altered or replaced without the need for specialised skills or equipment, thereby reducing down time when performing maintenance. The flexibility of wood allows it to flex repeatedly with little fatigue (Manalo 2011). The flexibility of wood also acts as a dampener for vibration transfer from the steel wheels on the rail to the bridge support structure causing audible noise. Noise from a passing train can be amplified by the bridge structure and it is important to take this into consideration especially in urban areas. The reduction in noise levels with effective dampening can be as much as 10db, therefore, the natural characteristic of flexibility found in wood is important (Poisson & Margiocchi 2006).

A major disadvantage of wood, from a structural point of view, is its susceptibility to fire. Fire is one of the most severe hazards that any built infrastructure may face. The increase in transported hazardous materials such as flammable materials, spontaneously combustible materials as well as corrosive materials is often considered safest when transported by rail (Garlock et al. 2012). The potential for major infrastructure cost due to a bridge fire caused by a transport accident, or even lightning strike is a reality.

The other main disadvantage of wood is that it has a limited life span due to deterioration caused by the natural processes of microbiological decay, insect attack, as well as mechanical fatigue (Adams 1991). Micro-organisms thrive in the right environment and the combination of bridge transoms made of wood with its natural bark defence removed, exposed to the weather, which introduces moisture and oxygen, provides an excellent habitat for these micro-organisms to thrive. The most serious kind of microbiological decay is caused by fungus, as it causes rapid structural failure. The most destructive and common form is brown rot (Monrroy et al. 2011). An example of failure due to fungal attack is shown in Figure 5. Brown rot feeds on the cellulose in the wood which comprises nearly 50% of the timber structure, without cellulose the wood has no ability to carry load (Xu & Goodell 2001). Fungal attack accounts for more than 50% of all railway sleeper failures (Ferdous & Manalo 2014).



Figure 5: Failure due to fungal attack (Ferdous & Manalo 2014)

The next most common form of failure for wood is splitting, which accounts for around 10% of railway sleeper failures. The natural process of timber swelling and shrinking when the timber equilibrates to the surrounding moisture conditions can cause horizontal splitting in the wood which seriously reduces the wood's strength (Akbiyik, Lamanna & Hale 2007). End splitting is a combination of swelling and shrinking along with transverse shear loading of the timber causing the planes of flexure of timber fibres to move and become separated. End splitting is shown below in Figure 6.



Figure 6: End Split (Ferdous & Manalo 2014)

The other major cause of sleeper failure is insect attack, in particular termites. Termites account for 7% of sleeper failure (Ferdous & Manalo). Termites feed on the cellulose in the wood, and as with fungus attack, without cellulose the wood has no ability to carry loads. An example of the extent that termite can attack affected wood is shown below in Figure 7.



Figure 7: Termite affected wood

2.2.1. Hardwood

Hardwood used for transoms, on average, have a lifespan of 20 years (Ferdous & Manalo 2014) and when the transom can no longer carry a load it is required to have maintenance to either renew or replace it. The life span of 20 years has largely come about through the use of Creosote to pressure treat the wood and help prevent fungal and insect attack (Bolin, Christopher & Stephen 2013). Creosote is a mid-heavy distillate of coal tar which contains large amounts of polycyclic aromatic hydrocarbons (PAH) and is widely used as a wood preservative (Ikarashi, Kaniwa & Tsuchiya 2005). Although the use of creosote has improved the lifespan of hardwood sleepers, its use has presented some problems when it comes to the disposal of expired sleepers. The EPA has recommended that creosote treated sleepers not come into direct contact with skin, not be used for firewood, and not be used for garden edging due to some PAH's being a potential human carcinogen (Ikarashi, Kaniwa & Tsuchiya 2005). To avoid end splitting in bridge transoms, the use of cross ties with a greater width and depth is used which reduces the overall transverse shear and the likelihood of failure due to end splitting. The use as transom decking is limited due to wood being unavailable in sizes suitable for use as a panel.

2.2.2. Softwood

Softwood of sufficient cross section has been used for rail cross ties, but due to difficulty of penetrating the wood with chemical treatments tends to have a smaller life span than hardwood (Vinden, Torgovnikov & Hann 2011). Hardwood transmits sap via its cellular structure which allows for easy treatment with creosote and other treatments (Vinden, Torgovnikov & Hann 2011). Softwood, however, conducts its sap through the use of tracheids which do not easily transmit chemical treatments. Without treatment softwood is more susceptible to fungal and insect attack (Webb 2005). According to (Arema 2003), softwood cross ties are inferior at spike holding and preventing gauge spread which eliminates them being used as bridge ties due to the potential for the track to move through lack of spike holding.

2.2.3. Plywood

The use of plywood as a rail sleeper is limited due to its classification as class 3 product (exterior exposure without ground contact) (Van den Bulcke et al. 2011). Due to rail sleepers having ground contact, plywood is excluded as a potential product. Plywood has been investigated and approved for application as vehicular bridge decking (ARTC 2008) and also investigated and approved for use as a ballast deck where the plywood is the material used to construct the box that contains the ballast that the rail and sleepers are placed in (ARTC 2008). Plywood has similar susceptibility to plain wood in terms of fungal and insect attack and thus has a similar lifespan. Due to plywood being made from laminations of timber shaved from the circumference of trees it has the ability to be manufactured in dimensions suitable for use as transom decking.

2.3. Concrete

Advances in concrete design in the 50's enabled the widespread implementation of concrete as a sleeper material. Approximately 500 million prestressed sleepers (containing stressed steel wires) worldwide are currently in use (Ferdous & Manalo 2014). Concrete is quite resilient, with a longer expected life than wood sleepers of 50 years. Due to concrete's natural limitation of weakness in tension, the dimensions of concrete sleepers must be increased to meet the required shear and

bending strength when used as a bridge cross tie with offset rails. The increased size renders it unusable as a replacement material for existing track ties made from wood.

The use as rail bridge transom decking is limited due to the dead loads encountered when of sufficient size to cope with the open deck bridge designs bending moments (Ngo et al 2013). Concrete is also very inflexible, and will transfer vibration noise from the rail to the bridge structure if the use of an absorbing pad is not used (Arema 2003). Concrete has been used as a type of direct fix rail bridge decking but mainly for light rail, and only for new installations (Duan 1999). These factors all add up to making concrete decking unsuitable as a replacement of existing bridge transoms.

2.4. Steel

Steel has been developed for use as a regular rail sleeper in Australia with up to 17% of all rail sleepers being made from steel (Manalo, 2011). Steel has been used as rail bridge cross ties in the form of I beams, however, the use actively transfers vibration noise to the substructure of the bridge (Hay 1982). Steel is susceptible to corrosion, especially around salty environments like coastal regions. Steel is also susceptible to fatigue cracking due to repeated stress cycles (Ferdous & Manalo 2014). Information on the use of steel as a transom decking material is very limited indicating that its use is quite limited. Due to the low forces involved, steel has been used as a decking over existing bridge cross-ties in order to create a safe walking platform. The cost and weight of steel in sizes suitable as transom decking prohibits its use.

2.5. Need for new type of sleeper

From the information provided it is apparent that all current alternatives for existing rail bridge cross ties have trade-offs. Wood has been the main stay of railway bridge transoms for such a long time for the simple reason that no other material currently provides all the necessary positive qualities of wood without providing negative qualities. As the purchase cost of large sized hardwood increases, the lifetime cost comparison of newly developed materials becomes more viable, thus, research into engineered materials such as fibre composites has become more popular (MCKAY 2013). Fibre composite materials can be engineered with material properties based on the required application, and have good durability requiring little in the way of maintenance (Manalo, 2011).

2.6. Composite sandwich structure

A composite sandwich is a type of laminate made up of more than 1 type of material and combined in a way to make best use of properties of the constituent materials. Typically a composite sandwich will have high strength but thin and dense skin material laminated (Glued) to a lower strength but low density and thick core material (ASM, 1999). The skins act to provide bending strength, whilst the core reduces overall weight and provides shear strength.

A particular unique fibre composite sandwich panel has been developed by a company in Toowoomba. The skins at the top and bottom are biaxial (0/90) layers of glass fibre. The core consists of a modified phenolic material (phenol formaldehyde resin) which uses plant oils for creation of the resin and mimics the properties of balsawood (often used for the core of composite sandwiches). The panel is made via an automated process and can be designed for various thickness combinations of skin and core as well as various dimensions of width and length. Due to the types of

uses the panel is currently being implemented as, the production of the panels is based on thicknesses (2 skins and 1 core) of 20mm.

Due to the use of plant based oils for the resin, the panels are more environmentally friendly and store carbon in the core of the panel. The sandwich manufacturing process uses 1/7th of the energy to produce compared to the production of concrete and steel. The strength and stiffness is comparable to that of hardwood but the panel is waterproof, fire resistant and not susceptible to rot or insect attack which gives a lifespan of 100 years (Loccomposites).

2.6.1. Properties

A study by (Manalo, et al, 2012) performed tests to characterize the properties of the skin and core of the fibre composite sandwich panel. 3 point bending, tensile and shear tests were performed to determine the compressive, tensile, and shear strength of the skin and core as well as the young's modulus and shear modulus. The manufacturer describes the panel as having similar workability to that of hardwood in that the panel can be drilled and worked with the same tools as that of hardwood with the same tools as used for wood.

The panel was found to behave in an isotropic linear elastic manner, except for the core material which exhibited a non-linear behaviour under compression. The core failed in tension with a much lower strength to that under compression, in a similar way to concrete, which enables the use of linear-elastic behaviour analysis when investigating the bending stresses for this project.

2.6.2. Applications

The sandwich panel has reached AS4858 accreditation as a waterproof membrane enabling its use in such areas as walkway decking in coastal areas, balcony decking, pedestrian bridge decking and bathroom panelling. Larger load uses have included a site access bridge decking for dump trucks over an existing creek, and high performance rail turnout sleepers (Manalo, 2011).

2.7. Conclusions

The particular requirement of a rail bridge transom and the natural properties of wood have made it the material of choice for rail bridge transoms. The scarcity of material with similar properties to wood has made the replacement of hardwood difficult. The properties of the new fibre composite sandwich being similar to those of hardwood and with the ability to produce in quantities needed naturally leads to its application as a potential rail bridge decking, and more so when the life span of the new material is considered. Further study of the suitability of the panel is present in the following chapters.

Chapter 3 - Methodology

3. Methodology

In order to determine the suitability of the fibre composite sandwich to fulfil the requirements of that of a rail bridge transom deck, the loadings, bending moment and shear must be calculated for a passing train. Some assumptions have been made to simplify the task of load calculations. Assumptions are discussed in the following sections along with the static bending moments and shear for a standard hardwood bridge transom.

3.1. Track design

3.1.1. Rail curvature

To enable a simpler analysis of bridge loads, it was decided that the rail design under consideration will be a single track and straight. A straight single track eliminates interaction between track directions, and eliminates lateral forces due to curvature (AS5100).

3.1.2. Gauge

According to (Mills 2010) the track gauges throughout Australia consist of the following:

- Standard Gauge 4 feet 8^{1/2} inches (1435 mm)
- Broad Gauge 5 feet 3 inches (1600 mm)
- Narrow Gauge 3 feet 6 inches (1067 mm) and 2 feet 6 inches (762mm)

For this project the broad gauge of 1600mm will be used, purely for ease of calculation, further explanation follows.

3.1.3. Cross Ties

The main dimension that will contribute to bending moment is rail offset to the cross tie support. The rail is offset by a maximum of 250mm, but usually less, to the bridge girder (MCKAY 2013). The loading applied at this offset causes the shear and moment forces in the cross tie. The worst case distance of 250 mm will be used and as such will provide the maximum shear and bending moment ever expected for a cross tie.

The total length of the cross tie between supports will be set using the standard gauge of 1600mm + 500mm (250 mm either side of rails) for total girder spacing of 2100 mm. This length will be tested and the bending moment and shear force will be calculated. Other dimensions of the transom will be assumed the same as other bridge cross ties 209 x 290 mm (Esveld 2001)

3.2. Track Loads

According to Australian standards for bridge design AS5100 (StandardsAustralia 2004) section 8 for rail bridges dictates that unless otherwise specified by the railway authority, bridges shall be designed for the load classified as 300LA.

3.2.1. 300LA track Load

Section 8.2 of AS4100 details the 300LA load, it explains that the 300LA load is a designation for loads applied due to groups of vehicles with four axles each having a load of 300kN, and spacing for axles of 1.7m, 1.1m and 1.7m. An additional load of 360kN is added 2 metres in front of the first axle to simulate the coupled locomotive. The system is illustrated in Figure 8.

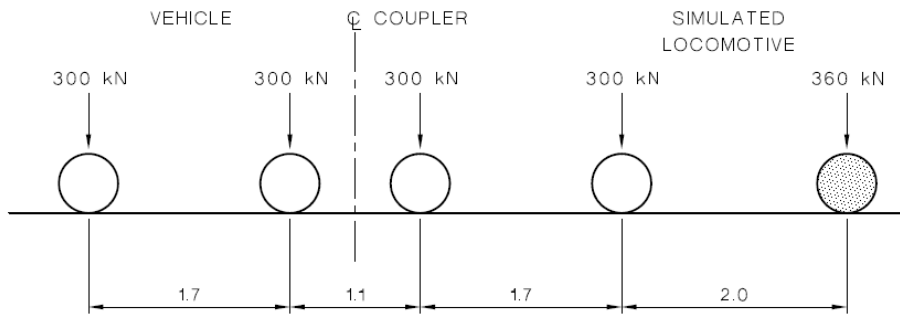


FIGURE 8.2(A) 300LA RAILWAY TRAFFIC LOADS—AXLE LOADS

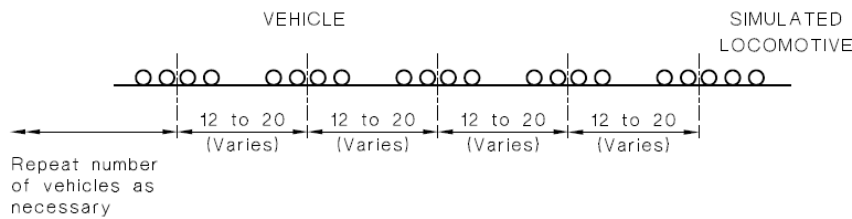


Figure 8: 300LA load system (AS 5100)

Section 8.3 deals with multiple track factors which have been excluded for this project.

Section 8.4 deals with the Dynamic Load Allowance in which Clause 8.4.1 states “The dynamic load allowance (α) for railway live load effects shall be a proportion of the static railway live load, and shall be calculated by the methods specified in this clause”. The method goes on to state that the value is the same for steel concrete or composite construction. The value of α is dependent on the characteristic length (L_α) and a distinction is made between different methods of supporting the track, i.e. with ballast or transom top structure.

The dynamic load allowance applies to both the ultimate and serviceability limit states. The design action is equal to:

$$(1 + \alpha) \times \text{the load factor} \times \text{the action under consideration}$$

Section 8.4.2 determines the characteristic length (L_α) for bridge superstructures, as we are dealing with cross-ties, which are not part of the superstructure, this section does not apply.

Section 8.4.3 deals with dynamic load allowance for bending effects.

Sub-section 8.4.3.2 deals with open deck spans and spans with direct rail fixation. This is the section for rail transoms. The dynamic load allowance (α) is listed in table 8.4.3.2. For lengths greater than 2.0 metres the load allowance (α) is calculated from the equation given in Table 1.

TABLE 8.4.3.2
VALUES OF α FOR BENDING MOMENT
FOR OPEN DECK SPANS AND SPANS
WITH DIRECT RAIL FIXATION

Characteristic length (L_α) m	Dynamic load allowance (α)
≤ 2.0	1.6
> 2.0	$\frac{2.16}{L_\alpha^{0.5}} - 0.17$

NOTE: The value of α shall not be less than 0.

Table 1: Values of Alpha (AS5100)

The required transom length is 2.1 metres (gauge 1600 + 2 lots of 250mm offset), so from equation 2 of AS5100 table 8.4.3.2, α equals 1.559. This value will be taken as 1.6, as that given for characteristic length ≤ 2.0 due to very small rounding.

The next section 8.4.5 deals with other load effects, namely; shear, torsion and reactions. The load allowance (α) for shear, torsion and reactions is taken as 2/3 of the value for bending moment.

section 8.5.2 states "Timber bridge transoms shall be designed on the assumption that the maximum wheel load on each rail shall be distributed equally to all transoms or fractions thereof within a length of 1.2m, but shall not be greater than three transoms, and the load shall be applied with a dynamic load allowance of 1.0".

According to (RailCorp 2015) Table 2, spacing of transoms may be determined from the supplied table.

Girder centres spacing (mm)	Transom spacing (mm)	Horizontal alignment of track (Radius m)	Minimum transom thickness (mm)
2000	500 - 550	> 800	170
		≤ 800	200
	600	> 800	190
		≤ 800	210
2100	500 - 550	> 800	190
		≤ 800	220
	600	> 800	200
		≤ 800	220

Table 2: Transom Spacing (Railcorp 2015)

As previously determined, the design girder spacing is 2.1 metres, the track is straight (radius > 800), and the standard transom thickness is 290mm which allows for a maximum transom spacing of 600mm.

According to section 8.5.2 of AS5100, the 360 kN load will be spread over 1.2 metres which equates to 2 transoms spaced at 0.6 metres. This spacing effectively halves the axle load to 180 kN per transom. There are 2 wheels per axle requiring each rail to support half the axle load. The total load is therefore 90 kN per rail per transom.

TABLE 8.8(A)
LOAD FACTORS FOR
DESIGN RAILWAY TRAFFIC LOADS

Loads	Limit state	
	Ultimate	Serviceability
300LA railway traffic load	1.6	1.0

Table 3: Load Factors (AS5100)

Table 3 above lists the design traffic loads. The table shows that the 300LA load has an ultimate limit state factor of 1.6 and a serviceability limit state of 1.0. Shown Below

The load per rail can now be determined:

Previously $(1 + \alpha) \times$ the load factor \times the action under consideration ($\alpha=1.6$) (Load Factor = 1.6)
(Action = 90kN)

Therefore the load per rail is now $2.6 \times 1.6 \times 90 = 374.4$ kN.

3.3. Bending Moment and Shear

3.3.1. Bending Moment

The static wheel load is now known to be 374.4 kN. From statics, the bending moment can be calculated at the maximum distance of 250mm. The bending moment is therefore:
 $374.4 \times 0.25 = 93.6$ kN.m

The modulus of elasticity of wood sleepers varies significantly, but a study by (Ticoalu, Aravinthan & Karunasena 2008) concluded that hardwood sleepers had a mean modulus of 16606 MPa. I have used this value in the strand7 software to represent an average transom. Results of static bending moments and shear force are shown below for the 300LA load.

3.3.2. Shear

As previously described, the shear dynamic load allowance (α) is $2/3$ of the value for bending moment.

Therefore the dynamic allowance is $2/3 \times 1.6 = 1.0667$

The design action is therefore $1 + 1.0667 \times 90 = 297.6$ kN

Shear is now able to be calculated from statics as being 297.6 kN

3.3.3. Conclusion

The diagrams for statically loaded rail transoms are shown below in Figure 9 and Figure 10. The Bending moment of 93.6 kN.m and shear force of 297.6 kN will be used to determine the dimensions required for the proposed fibre composite sandwich panel.

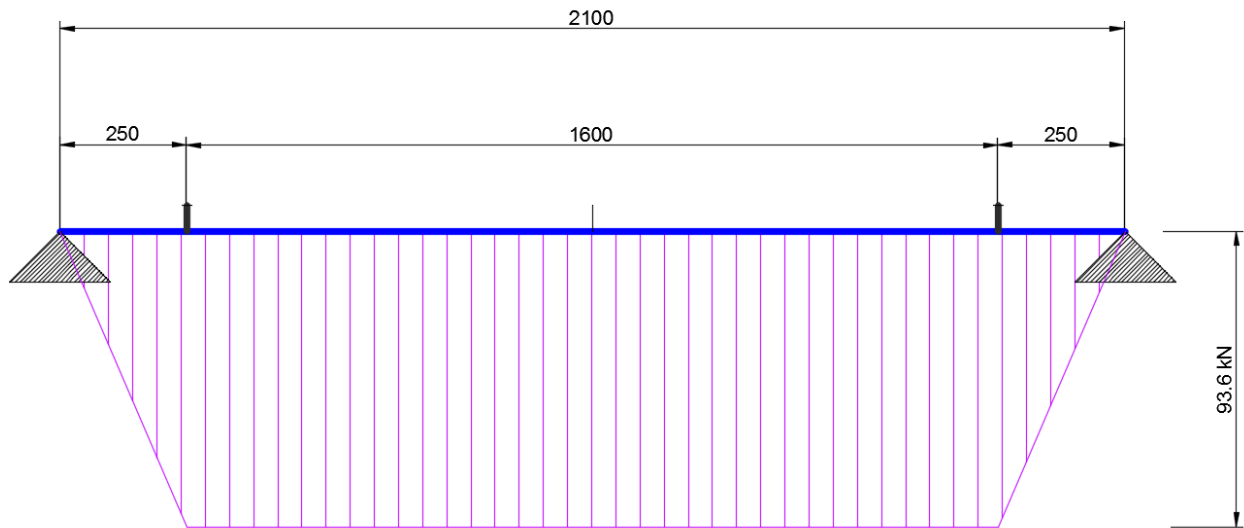


Figure 9: Bending Moment Diagram

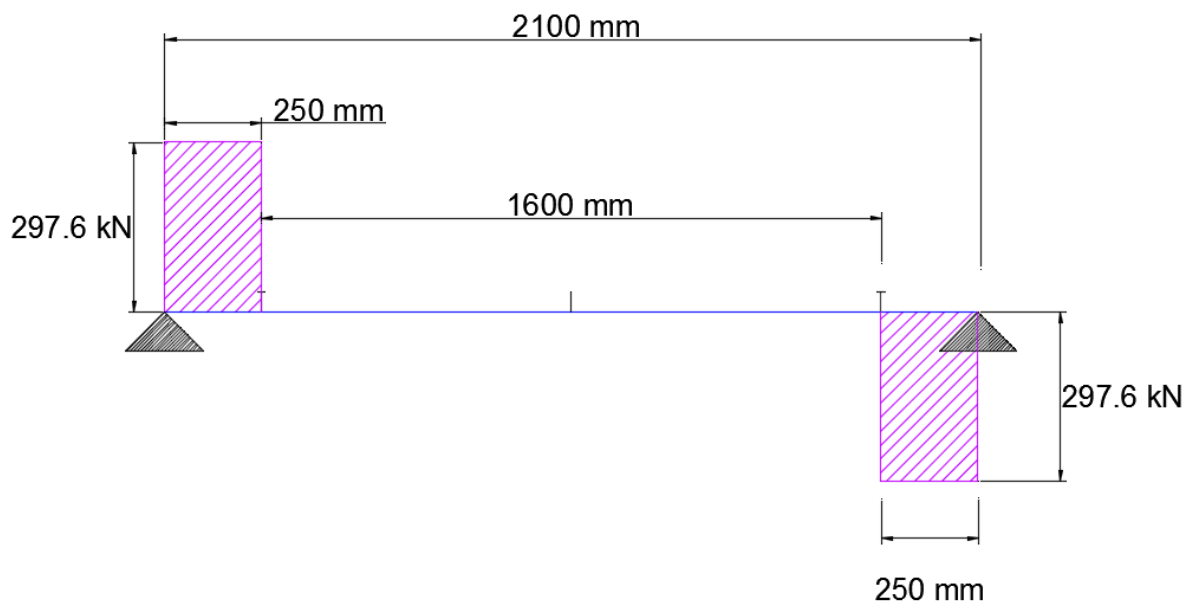


Figure 10: Shear Force Diagram

Chapter 4 - Bridge Transoms

4. Fibre Composite transom dimensions

The sandwich panel will be theoretically designed in flatwise and edgewise single layer, as well as flatwise and edgewise multiple layers to determine the configuration that best meets the static bending moment and shear force requirements for a transom of dimensions 290mm (wide) x 209mm (high). Example of positions is shown below in Figure 11

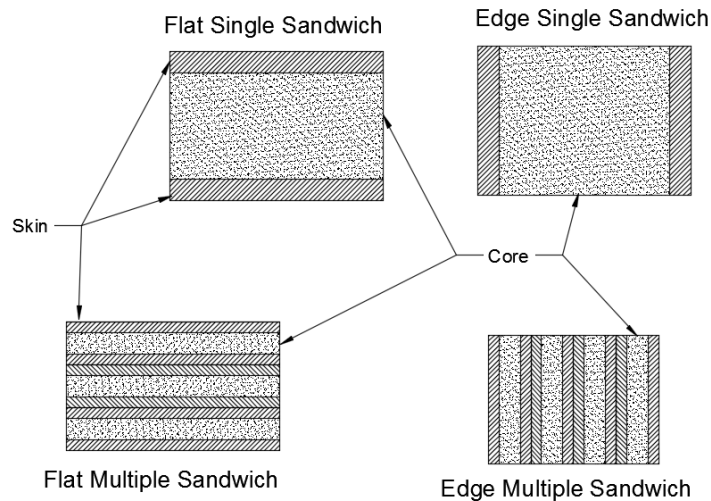


Figure 11: Panel Layout and Orientations

The most suitable arrangement for a panel of a required width shall then be tested using finite element analysis software package Strand7 (Student edition) to determine the suitability of the panel as a transom deck.

4.1. Single Sandwich

4.1.1. Introduction

The flat single sandwich will be designed for the maximum expected bending moment of 93.6 kN. The calculated bending of the beam is in positive moment convention concave upwards as shown below in Figure 12. The figure also shows the neutral axis, and the section of the beam in compression and tension above and below the neutral axis.

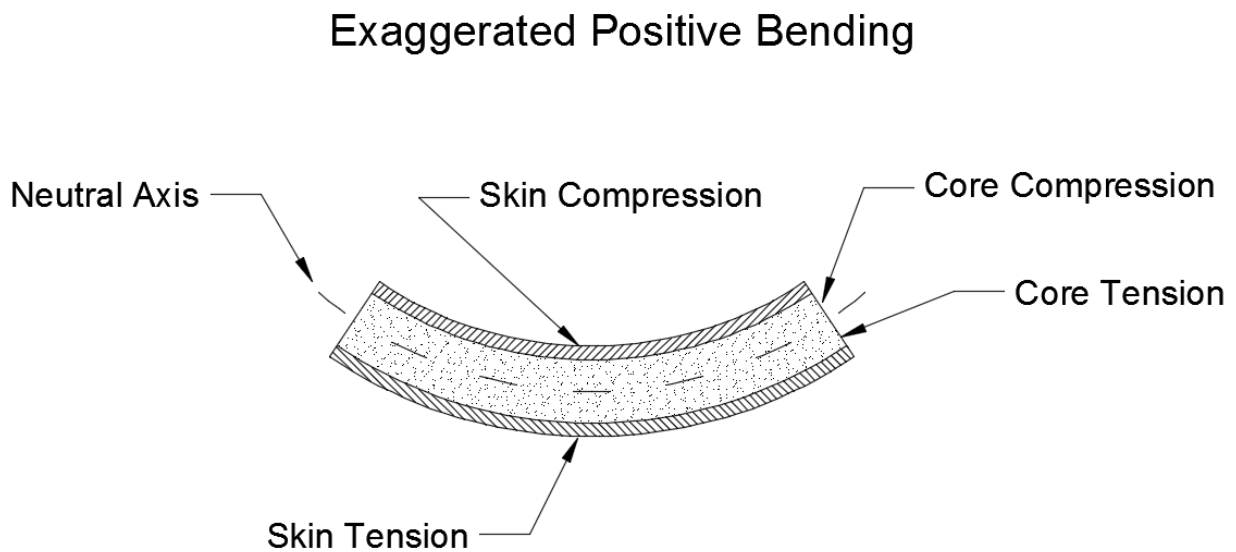


Figure 12: Positive Bending

From the comprehensive study by (Manalo, Aravinthan & Karunasena 2010) the properties for the skin and core of the fibre composite sandwich being investigated is listed in Table 4. The data was developed with the assumption that the skin and core behave in a linear elastic way. Therefore for the purpose of this investigation, it is also assumed that the skin and core behave in a linear elastic way and abide to Hooke's law.

Property	Skin	Core
Tensile strength, MPa	247.2	5.97
Compressive strength, MPa	201.8	21.4
Shear strength, MPa	27.8	4.5
Young's modulus, GPa	12.82	1.33
Shear modulus, GPa	2.47	0.52
Strain at peak in tension, %	1.87	0.61
Strain at peak in compression, %	1.56	1.60
Strain at peak in shear, %	2.38	0.81

Table 4: Properties of Core and Skin of Sandwich

4.1.2. Design for Bending

According to Hooke's law (Ivanoff 1995) :

1. There is no stress at the neutral plan
2. The maximum tensile stress occurs in the extreme fibre on the convex side of the beam.
3. The maximum compressive stress occurs in the extreme fibre on the concave side of the beam.

The equation which represents the relations above is shown below in equation 4.1:

$$\sigma = \frac{MY}{I} \quad (4.1)$$

Where σ = Bending stress in Mpa

M = bending moment at a given cross section N.mm

Y = the distance from the neutral plane to a particular fibre, in mm

I is the moment of inertia of the cross-section mm⁴

Utilising Hooke's law, the skin and core thickness must be designed in order to prevent the layers above the neutral axis exceeding the Maximum compressive stress of 201 Mpa for the skin and 4.25 Mpa for the core. The lower sections similarly must not exceed the maximum tensile stress of 201 Mpa for the skin and 1.94 for the core.

It is universally accepted that the skin of a fibre composite sandwich supports the bending force, and the core supports the shear force (Bekuit et al. 2007).

Due to the differing modulus of the skin and core, the beam has its equivalent flexural stiffness calculated (EI). The flexural stiffness allows the calculation of the equivalent strain at the location required, which can then be multiplied by the particular materials modulus to determine stress. An example for the equation for the skin stress is shown below in equation 4.2. The same equation is used for the core but for σ_s and using term E_c .

$$\sigma_s = \frac{MY}{EI} \cdot E_s \quad (4.2)$$

From the sandwich structure properties in Table 4, it can be seen that the skin has a higher tensile strength than compressive strength, so it can be reasonably assumed that the skin will fail under compression before tension, therefore the upper skin of the sandwich in figure 9 will fail first as it is in compression.

The core, similarly, supports a much higher compressive stress 21.4 Mpa compared to its tensile stress 5.97 Mpa; therefore it is also assumed that the core will fail under tensile stress before compressive stress.

According to (Manalo 2011) the contribution of both the flexural stiffness of both the core and skin for this particular composite sandwich should be considered for bending and shear.

The flexural stiffness of the sandwich was developed from the flexural stiffness of the contributing parts (bottom skin, core and top skin) about the neutral axis as shown below in Figure 13

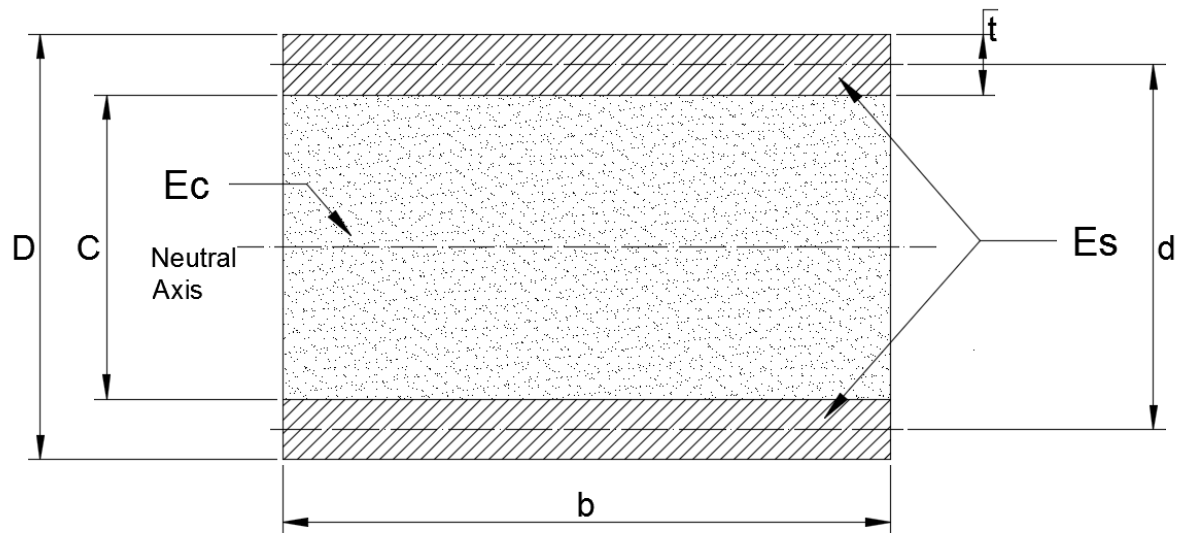


Figure 13: Flat Sandwich Moduli

From Figure 10:

- Ec is the modulus of elasticity of the core d=D-t
- Es is the modulus of elasticity of the skin. C=D-2t
- d is the distance between the centroids of the skin
- C is the core depth
- D is the depth overall
- t is the skin thickness.

The below equation 4.3 is used to calculate the flexural stiffness, the derivation of the formula is shown in Appendix A.

$$EI = E_c \frac{bc^3}{12} + E_s \left[\frac{bt^3}{6} + \frac{btd^2}{2} \right] \quad (4.3)$$

Knowing that:

$$c = D - 2t$$

&

$$d = D - t$$

The equation is re-arranged in terms of known dimensions b and D as follows:

$$\therefore EI = E_c \frac{b(D - 2t)^3}{12} + E_s \left[\frac{bt^3}{6} + \frac{bt(D - t)^2}{2} \right]$$

For the first trial a thickness of $t = 15\text{mm}$ was used along with the existing known overall dimensions (mm) of $b=290$ $D=204$ making the core thickness $c = 209 - (2 \cdot 15) = 179$ mm & $d = 209 - 15 = 194$

$$EI = 1350 \left[\frac{300 * (179)^3}{12} \right] + 14280 \left[\frac{290 * 15^3}{6} + \frac{290 * 15(194)^2}{2} \right]$$

$$EI = 1350[131700600] + 14280[163125 + 77693175]$$

$$EI = 1350[131700600] + 14280[163125 + 77693175]$$

$$EI = 1.2338 \times 10^{12}$$

From this the stress at the extreme fibres of the skin above the neutral axis can be determined from the equation 4.2:

$$\sigma_s = \frac{MY}{EI} \cdot E_s$$

$$\sigma_s = \frac{93.6 * 104.5}{1.2338 \times 10^{12}} \cdot 12820$$

$$\sigma_s = 101.64 \text{ Mpa}$$

The stress in the skin of 101.64 is less than the maximum compressive stress of 201.8 Mpa, but a check must be done to ensure that the core of the sandwich below the neutral axis does not exceed the maximum tensile stress allowable of 5.97 Mpa.

The panel has the same equivalent flexural stiffness (EI), but this time the distance from the neutral axis downwards to the edge of the skin $Y = (C/2)$ where $C = D - 2t$, making $Y = (D/2) - t = (209/2) - 15 = 89.5$ mm.

The stress calculated using equation 4.4 below.

$$\sigma_c = \frac{MY}{EI} \cdot E_c \quad (4.4)$$

$$\sigma_c = \frac{93.6 \times 10^6 * \left[\left(\frac{209}{2} \right) - 15 \right]}{1.2338 \times 10^{12}} \cdot 1330$$

$$\sigma_c = 9.03 \text{ Mpa}$$

Clearly 9.03 Mpa is larger than the maximum of 5.97 Mpa, therefore the core will fail in tension and the design is not feasible.

An excel spreadsheet was developed using the above equations which enabled the manipulation of the thickness of the skin while automatically calculating the stresses in both the skin and core at their respective extremes. From this spreadsheet a design for thickness of skin and core could be determined.

During 4 point testing performed by (Manalo 2011) the core presented tensile cracking at the expected stress, but the skin in tension prevented the cracks widening further and causing premature failure of the beam. The beam only failed when the top skin failed due to compression indicating that core cracking does not result in instant failure of the beam, however, for this project the beam design shall be such that tensile cracking of the core does not occur to ensure that the core remains fully intact during expected loads and any failure due to overload will present as a ductile failure.

4.1.3. Design for shear

The prediction of shear strength according to (Manalo et al, 2010), and confirmed with physical testing, that in a flat layout sandwich shear failure was due to shear failure of the core. It was also determined that an equation using the term N_G , which represent the ratio of the skin shear modulus to that of the core, better represents the shear strength of the sandwich panel. Equation 4.5 below was developed to calculate the core shear stress due to shear load.

$$\tau_c = \frac{P_c}{(2t_c n_g + t_c)D} \quad (4.5)$$

Where P_c is the shear load applied.

The following calculations for initial size of $b = 290$ mm $D = 209$ mm and $t=15$ mm is shown

$$\tau_c = \frac{297.6 \times 10^3}{\left(2 * 15 * \frac{27.8}{4.5} + 15\right) 209}$$

$$\tau_c = 7.1 \text{ Mpa}$$

It is seen then that shear stress is greater than the allowed 4.5 MPa therefore the core will fail in shear. An excel spreadsheet is used to calculate the shear based on the known dimensions and trial thicknesses of skin material with the results presented in section 4.1.4 below.

4.1.4. Flatwise Results

From the excel spreadsheet the thickness of the skin was adjusted until the tensile stress in the core was below 5.97 Mpa. At the same thickness the shear in the core was calculated and found to be below the maximum of 4.5. Results are shown below in Table 5.

Table 5: Single Sandwich Flatwise

Results (Single Sandwich Flatwise)						
Skin Depth (mm)	Flexural Stiffness EI (x10 ¹²)	Stress (Skin) (Mpa)	Stress T (core) (Mpa)	Shear Core (Mpa)	Max Bean Shear stress (kN)	Max Beam Bending Moment (kN.m)
24.3	1.67	74.92	5.97	4.39	305.23	126.05

4.2. Edge single sandwich

4.2.1. Design for bending

The single sandwich orientation edgewise uses the similar process of design of thickness of the beam. Due to the symmetry above and below the neutral axis the flexural stiffness calculation is easier and shown below in equation 4.6.

$$EI = E_c \frac{CD^3}{12} + E_s \frac{tD^3}{6} \quad (4.6)$$

The flexural stiffness is again 1 lot of second moment of area of the core times the modulus of elasticity of the core, plus 2 lots of second moment of area of the skin times the modulus of the skin. In this arrangement, however, the skins are not offset about the neutral axis due to there being equal amounts of skin above and below the neutral axis along with equal amounts of the core above and below the neutral axis. This is demonstrated in the figure below Figure 14

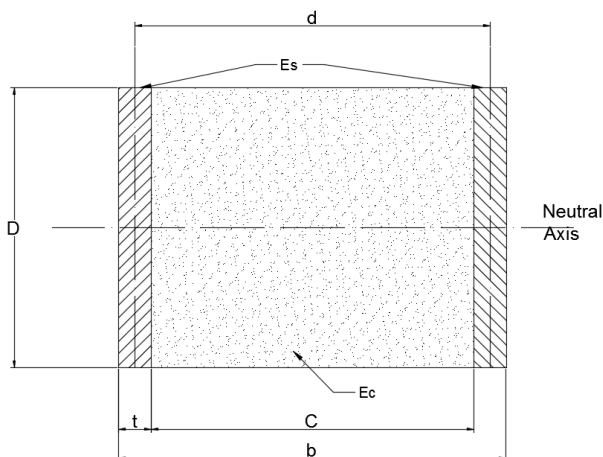


Figure 14: Edgewise layout

Using the same dimensions of 290mm wide by 209 mm high, it can be seen that the core now covers the full height of the beam and it is expected that the beam will fail by tensile failure of the core first. The beam is therefore checked for tensile stress in the lower extremities of the core as follows using the same initial skin thickness of 15mm:

$$EI = 1330 * \frac{(290 - (2 * 15)) * 209^3}{12} + 12820 * \frac{15 * 209^3}{6}$$

$$EI = 5.56 \times 10^{11}$$

Stress in the core is then

$$\sigma_c = \frac{MY}{EI} \cdot E_c$$

Where Y=height above the neutral axis (209/2 = 104.5 mm)

$$\sigma_c = \frac{93.6 \times 10^6 * 104.5}{5.56 \times 10^{11}} \cdot 1330$$

$$\sigma_c = 23.4 \text{ Mpa}$$

The tensile stress in the core is larger than the maximum of 5.97 MPa and will cause tensile failure of the core. The equation was again used in conjunction with an excel spreadsheet to enable fast calculation of various thicknesses of the skin; unfortunately it was found that skin thickness would need to be 107 mm each in order to reduce the tensile force in the extreme lower fibres of the core below 5.97 Mpa. The reason for this is that with the skin material in the edgewise orientation, there is less material to provide tensile and compressive resistance at the points of greatest stress (top and bottom), therefore the flexural stiffness is reduced and the beam will bend more developing more strain and therefore tensile stress in the core at the bottom of the beam.

4.2.2. Design for Shear

As with flatwise orientation, the edgewise orientation utilises an equation developed by (Manalo, 2011) shown below (4.7). In this orientation however the shear failure of the beam is caused by shear failure of the skin.

$$\tau_s = \frac{P_s}{\left(2t_s + \frac{1}{n_g} t_c\right) D} \quad (4.7)$$

For the initial skin thickness of 15mm and same dimensions of 290 mm (wide) and 209 mm (high)

$$\tau_s = \frac{297.6 \times 10^3}{\left(2 * 15 + \frac{1}{6.178} * 260\right) 209}$$

$$\tau_s = 19.75 \text{ Mpa}$$

The shear strength of the skin is 27.8 showing that this thickness of skin has enough shear strength despite the lack of core tensile strength. This result is interesting as it shows that the beam in this orientation has sufficient shear, even though the beam with equivalent skin thickness in the flatwise orientation did not. This shows that the skin is providing the shear in the edgewise orientation and due to the shear strength of the skin being much greater than that of the core, less material is needed to provide sufficient strength.

4.2.3. Edgewise Results

The results below in Table 6, shows that the thickness of skin required to reduce the core tensile stress below maximum constitutes nearly half the width of the beam. Accordingly the beam has huge shear strength capacity due to the skin having a larger shear capacity than the core.

Table 6: Single Sandwich Edgewise

Results (Single Sandwich Edgewise)						
Skin Depth (mm)	EI ($\times 10^{12}$)	Stress (Skin) (Mpa)	Stress T (core) (Mpa)	Shear Skin (Mpa)	Max Beam Shear stress (kN)	Max Beam Bending Moment (kN.m)
108.0	2.182E+12	57.48	5.96	6.25	1324.60	164.31

The use of this sandwich panel as a potential replacement for existing bridge transoms requires that it meet the same dimensions as that of existing transoms. In order to reduce the thickness required for the skin whilst maintaining the core below maximum stress the overall beam height must be increased. The beam is therefore deemed not to comply and will not be further investigated in a single sandwich edgewise layout. The increase in shear capacity of the beam in the edgewise layout due to the orientation of the skins will be further explored through the use of multiple laminate edgewise orientation which will be investigated in the next section.

4.3. Multiple Flatwise Sandwich

A study was performed by (Manalo, Aravinthan & Karunasena 2010) in which a full scale railway turnout sleeper was developed from laminated layers of the same fibre composite sandwich material this project is concerned with. Sandwich layers of approximately 20mm were used to construct several beam in both the flatwise and edgewise orientation. The beams were tested under 4 point static bending to destruction in order to study the failure behaviour and develop equation for predicting flexural strength and shear for the different configurations. Results indicated again that in the flatwise orientation the beams failed due to compressive failure of the topmost skin. In the edgewise orientation the beam failed in a ductile manner due to skins providing reinforcement to the core as it cracked and allowing a progressive compressive failure of the skins from the outer most layer towards the middle.

4.3.1. Multiple Flatwise Sandwich Design for Bending

The calculations for flexural stiffness is presented below for flatwise and edgewise orientation in equation 4.8 & 4.9, they again build on the standard equations presented in equations 4.3 and 4.6, but with multiple laminations

$$EI_{flat} = \sum_{i=1}^n \left[\left(\frac{Bt_s^3}{12} + Bt_s d_s^2 \right) E_s + \left(\frac{Bt_c^3}{12} + Bt_c d_c^2 \right) E_c \right] \quad (4.8)$$

$$EI_{edge} = \frac{nD^3}{6} \left(t_s E_s + \frac{t_c}{2} E_c \right) \quad (4.9)$$

d_s and d_c are the distances from the centroid of the skins and cores to the neutral axis of the section
 n is the number of laminations

Calculation is the same as that used for a single sandwich, except that the distances between the centroids of the skin and core t_s and t_c changes with each increase in laminations. An excel spreadsheet was developed to automate the calculation of the flexural stiffness by simply altering the overall dimension and thickness of the skin.

Maximum bending stress is then calculated using equation 4.4 modified for skin or core stress calculation. Assumptions made in the use of this equation by (Manalo, Aravinthan & Karunasena 2010) is that no inter layer slippage occurs, and that the laminated beam behaves as a solid section with perfect bonding.

The skin thickness was initially calculated based on the ratio of skin thickness to overall panel dimension used in (Manalo 2011) where the skin thickness was 1.792mm and overall panel dimension was 20mm giving a ratio of 8.96%. When the calculations were set up in the spreadsheet however the results showed that the core was developing too much tensile stress. The thickness was therefore manually changed in the spreadsheet to find the thinnest skin material to the nearest whole millimetre that still caused a core tensile stress below the maximum core tensile strength of 5.97 Mpa

The results for multiple layer flat layout laminated beam with varying numbers of sandwich layers is shown below in Table 7. The results also show the calculated flexural stiffness EI as well as skin stress, core stress, core shear and overall beam maximum bending moment and shear.

Table 7: Multiple Flatwise Layout

Laminations	2	3	4	5	6	7	8	9	10
Laminate Overall Height (mm)	104.5	69.6	52.2	41.8	34.8	29.8	26.1	23.2	20.9
Skin Thickness (mm)	24	19	16	13	12	10	9	8	8
Core Thickness (mm)	56.5	31.6	20.2	15.8	10.8	9.85	8.12	7.22	4.9
Overall Beam height (mm)	209	209	209	209	209	209	209	209	209
EI Beam (Nmm ²)(x10 ¹²)	1.70	1.78	1.90	1.90	2.06	2.00	2.05	2.05	2.24
Stress outer skin C (Mpa)	73.7	70.5	66.0	65.8	60.8	62.7	61.1	61.3	55.9
Stress most extreme core T (Mpa)	5.89	5.99	5.80	5.99	5.59	5.89	5.80	5.87	5.36
Max B.M (kN.m)	128	133	143	143	155	150	154	154	168
Core Shear Stress (Mpa)	1.45	1.28	1.18	1.16	1.08	1.10	1.08	1.08	0.99
Max Shear Beam (kN)	921	1043	1138	1151	1246	1219	1246	1246	1354
Laminations	11	12	13	14	15				
Laminate Overall Height (mm)	19.0	17.4	16.0	14.9	13.9				
Skin Thickness (mm)	7	7	6	6	3				
Core Thickness (mm)	5	3.41	4.07	2.92	7.93				
Overall Beam height (mm)	209	209	209	209	209				
EI Beam (Nmm ²)(x10 ¹²)	2.16	2.32	2.16	2.28	1.34				
Stress outer skin C (Mpa)	57.9	53.9	58.0	55.0	93.8				
Stress most extreme core T (Mpa)	5.61	5.22	5.67	5.38	9.45				
Max B.M (kN.m)	163	175	162	171	100				
Core Shear Stress (Mpa)	1.02	0.95	1.01	0.95	1.52				
Max Shear Beam (kN)	1313	1408	1327	1408	881				

The skin thickness for the beam with 15 laminates was adjusted to 3mm to replicate the thickness of skin used in the (Manalo, 2011) laminated beam test. For this beam it can be seen that the core stress exceeds the maximum of 5.97 by a significant amount and would cause core cracking which, stated earlier, is being avoided for safety reasons.

4.3.2. Multiple Flatwise Sandwich Design for Shear

$$\tau_c = \frac{P_F}{n \left(t_c + 2t_s \frac{G_s}{G_c} \right) b} \quad (4.10)$$

As shown in Table 7, the core shear decreases for even numbers of laminations, this is due to the odd numbers having the neutral axis through the centre of a laminate core.

4.3.3. Multiple Flatwise Sandwich Conclusion

From the data, it can be seen that with more laminations the beam has an increase in flexural stiffness. This is largely due to the increasing amount of skin material and its higher young's modulus. The overall amount of skin material is increasing whilst having a reduction in individual layer thickness due to there being, essentially, more skin due to each additional lamination introducing 2 more layers with only a slight reduction in thickness. Accordingly, when the beam reaches 3 laminations there is more overall skin material than core material.

According to (Manalo, 2011) the strength of a laminated flatwise sandwich when tested to destruction is governed by the compressive strength of the skin. When the beam is designed to prevent tensile failure of the core material however, the design seems to be governed by the tensile strength of the core.

From the results presented it is seen that, for a design with specific dimension and high loads, adding more laminations has a similar effect to increasing the skin thickness on a single sandwich. The increasing amount of skin material is also increasing the shear capacity of the beam due to its much higher shear capacity.

For interests sake, results presented below in Table 8, are for the same beam with an increase in height to 300mm. The same skin thickness for each lamination is maintained as well as the beam width. The results for up to 10 laminations are shown as a comparison.

Table 8: 300mm High Multiple Flat Sandwich

Laminations	2	3	4	5	6	7	8	9	10
Overall Dim (mm)	150	100	75	60	50	42.8	37.5	33.3	30
Skin Thickness (mm)	24	19	16	13	12	10	9	8	8
Core Thickness (mm)	102	62	43	34	26	22.8	19.5	17.3	14
Overall height (mm)	300	300	300	300	300	300	300	300	300
EI Beam (x10 ¹²)	3.95	4.03	4.25	4.23	4.55	4.40	4.51	4.49	4.89
Stress outer skin (Mpa)	45.5	44.6	42.3	42.5	39.6	40.8	39.9	40.0	36.7
Stress most extreme core Tensile (Mpa)	3.97	4.04	3.93	4.03	3.78	3.96	3.89	3.94	3.61

From these results it can be determined that with an increase in height of the beam, the core stress is reduced by around 32%. This is due to the increased flexural stiffness caused by the increased dimension of the core enabling the skins to be further away from the neutral axis and resisting more of the tensile and compressive forces. The results prove that in this particular case the core and skin material are not particularly suited for a beam with these combinations of shear and bending moment combined with specific dimension of height and breadth.

Another comparison is shown below in Table 9 for a wider beam section of 350 mm but with the same 209 mm height.

Table 9: 350 mm Wide Multiple Flat Sandwich

Laminations	2	3	4	5	6	7	8	9	10
Overall Dim	104.5	69.67	52.25	41.80	34.83	29.86	26.13	23.22	20.90
Skin Thickness	24	19	16	13	12	10	9	8	8
Core Thickness	56.5	31.66	20.25	15.8	10.83	9.857	8.125	7.222	4.9
Overall height	209	209	209	209	209	209	209	209	209
EI Beam ($\times 10^{12}$)	2.05	2.15	2.29	2.30	2.49	2.41	2.48	2.47	2.70
Stress outer skin (Mpa)	61.11	58.44	54.74	54.60	50.44	51.98	50.65	50.81	46.39
Stress most extreme core Tensile (Mpa)	4.88	4.96	4.81	4.96	4.63	4.88	4.80	4.87	4.44

It is also clear from these results that the width plays a part in reducing the core tensile stress, as the core tensile stress in this layout has been reduced from 5.89 in the original layout to 4.88, a reduction of 17%. This is again due to an increased amount both skin increasing the beam flexural stiffness. This will be further explored in chapter 5 and the design for a wide panel. Finite element modelling will be done on flatwise multiple laminate with 4 layers, as this is the maximum amount of layers with the skin still thinner than the core, which is a major design criteria for classification as a composite sandwich.

4.4. Multiple Edge Sandwich Design for Bending

The Flexural stiffness of the beam with multiple sandwiches oriented in flatwise uses equation 4.9 and is much simpler to implement for more layers being simply multiples of the EI for 1 layer. An excel spreadsheet was again utilised for calculation of the maximum stress developed at the extreme fibres of the skin and core. The results are presented below Table 10. It is clear that in order to reduce the maximum tensile stress in the core material the skin thickness must be such that there is actually less core material than skin material. One of the advantages of composite sandwiches is that they are relatively light for their strength; this is mostly due to the lower density of the core and larger amount compared to the higher density skin. The configurations needed in the edgewise layout requires more skin than core, and therefore would be heavy and difficult to manufacture.

Table 10: Multiple Edgewise layout

Laminations	2	3	4	5	6	7	8	9	10	11	12
Overall Dim (mm)	145	96.6	72.5	58.0	48.3	41.4	36.2	32.2	29.0	26.4	24.2
Skin Thickness (mm)	54	36	27	22	18	16	14	12	11	10	9
Core Thickness (mm)	37	24.67	18.5	14	12.3	9.43	8.25	8.22	7	6.36	6.17
Overall Width (mm)	290	290	290	290	290	290	290	290	290	290	290
EI (Nmm ²)(x10 ¹²)	2.18	2.18	2.18	2.22	2.18	2.25	2.25	2.18	2.22	2.22	2.18
Stress skin Top/Bot (Mpa)	57.4	57.4	57.4	56.5	57.4	55.6	55.6	57.4	56.5	56.5	57.4
Stress core Top/Bot (Mpa)	5.96	5.96	5.96	5.87	5.96	5.78	5.78	5.96	5.87	5.87	5.96
Shear Skin (Mpa)	6.25	6.25	6.25	6.16	6.25	6.07	6.07	6.25	6.16	6.16	6.25
Beam Max Shear (kN)	1324	1324	1324	1344	1324	1363	1363	1324	1344	1344	1324
Beam Max B.M (kN.m)	164	164	164	166	164	169	169	164	166	166	164

As described in the previous section, if the height dimension of the beam is increased then the tensile force in the core will reduce which will then allow a reduction in skin thickness. Due to the restricted beam height this is not possible. When the beam is designed as a panel, the increased width may lower the core maximum tensile stress; this will be further investigated in Chapter 5.

4.4.1. Multiple Sandwich Edge Layout Design for Shear

The calculation for shear is based on equation 4.11 developed by (Manalo, 2011). The calculations were performed in an excel spreadsheet with the results also presented in Table 8. Again it is clear that an edgewise layout provides substantial benefit from a shear perspective.

$$\tau_s = \frac{P_E}{n \left(t_c \frac{G_c}{G_s} + 2t_s \right) D} \quad (4.11)$$

4.4.2. Multiple Sandwich Edge Layout Conclusion

As with the flat layout, the beam needs more height to allow a combination of skin and core material that is feasible. The result for the shear in edgewise layout compared to the same amount of laminations in a flatwise layout shows an increase of 30%. Due to the increased shear in the edgewise layout a third combination is proposed with laminations glued in an edgewise layout and skin material added to the top and bottom. This orientation is investigated in the following section.

4.5. Combination Layout

The combination layout of edgewise laminated composite fibre sandwiches with flatwise glass fibre skins top and bottom is proposed and shown below in Figure 15

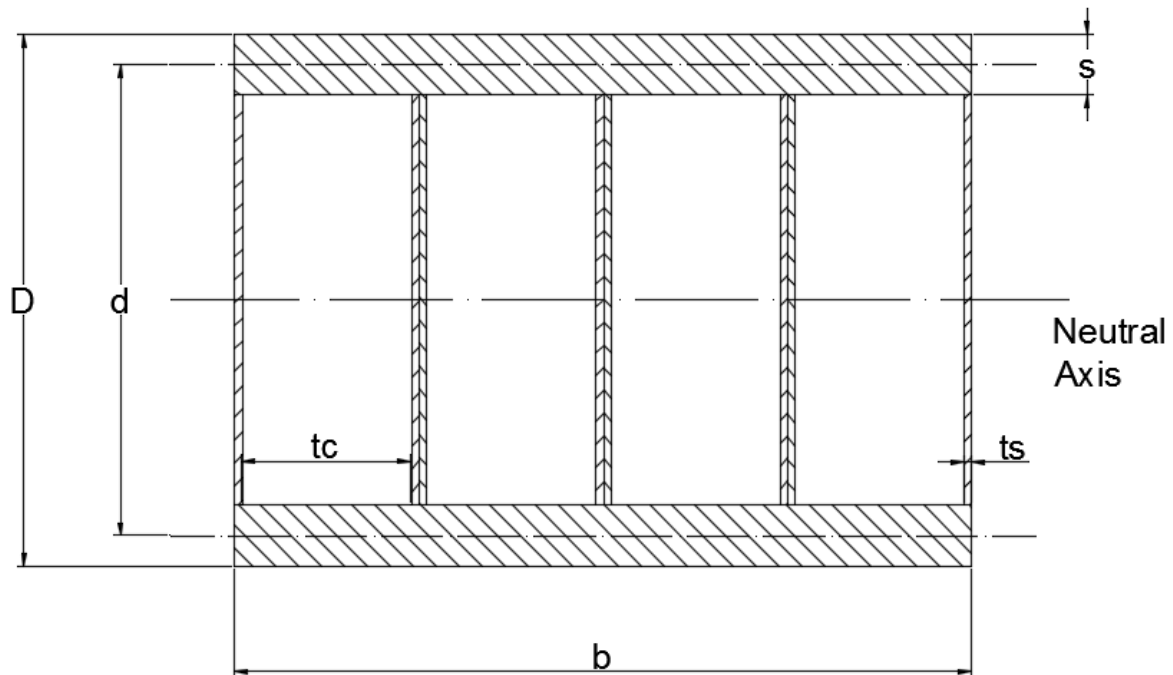


Figure 15: Combination Layout

It is hoped that this layout will provide the best of both multiple lamination layouts with the top and bottom flatwise skins carrying the majority of the bending stress, along with the edgewise sandwiches carrying the majority of the shear.

4.5.1. Combination design for bending

The equations 4.8 and 4.9 were adjusted and combined in order to calculate the flexural stiffness of the beam with various combinations of:

- Number of edgewise laminations
- Thickness of skin for edgewise laminations
- Thickness of skin on top and bottom of beam

The calculations were performed in an excel spreadsheet to speed up the adjustment of parameters.

4.5.2. Combination design for shear

As the beam had no core component on the top and bottom of the beam in a flatwise layout, and due to the fact that maximum shear is developed towards the middle of the beam, equation 4.11 was solely used to calculate the shear carried by the edgewise skins. The calculations performed in an excel spreadsheet for ease of adjustment.

4.5.3. Combination design conclusion

Results for combination arrangement are shown below in Table 11

Table 11: Combination Layout part 1

Laminations	2	3	4	5	6	7	8	9	10
Overall Dim	145	96.6	72.5	58.0	48.3	41.4	36.2	32.2	29.0
Lamination Skin Thickness	6	4	3	3	3	3	3	3	3
Core Thickness	133.	88.7	66.5	52.0	42.3	35.4	30.3	26.2	23.0
Overall Width	290	290	290	290	290	290	290	290	290
Top/Bottom Skin Thickness	24	24	24	24	24	24	24	24	24
Height	161	161	161	161	161	161	161	161	161
EI Edgewise skin & Core ($\times 10^{12}$)	0.23	0.23	0.23	0.25	0.27	0.30	0.32	0.35	0.37
EI top bottom Skin ($\times 10^{12}$)	1.54	1.54	1.54	1.54	1.54	1.54	1.54	1.54	1.54
EI Total ($\times 10^{12}$)	1.77	1.77	1.77	1.79	1.81	1.84	1.86	1.89	1.91
Stress skin Top/bot (Mpa)	71	71	71	70.0	69.1	68.2	67.3	66.5	65.7
Stress core top/bot (Mpa)	5.68	5.68	5.68	5.60	5.53	5.45	5.38	5.32	5.25
Shear Stress Skin (Mpa)	27.6	27.6	27.6	25.6	23.9	22.5	21.2	20.1	19.0
Laminations	11	12	13	14	15				
Overall Dim	26.3	24.1	22.3	20.7	19.3				
Lamination Skin Thickness	3	3	3	3	3				
Core Thickness	20.4	18.2	16.3	14.7	13.3				
Overall Width	290	290	290	290	290				
Top/Bottom Skin Thickness	24	24	24	24	24				
Height	161	161	161	161	161				
EI Edgewise skin & Core ($\times 10^{12}$)	0.39	0.42	0.44	0.47	0.49				
EI top bottom Skin ($\times 10^{12}$)	1.54	1.54	1.54	1.54	1.54				
EI Total ($\times 10^{12}$)	1.93	1.96	1.98	2.01	2.03				
Stress skin Top/bot (Mpa)	64.9	64.0	63.3	62.5	61.8				
Stress core top/bot (Mpa)	5.18	5.12	5.06	5.00	4.94				
Shear Stress Skin (Mpa)	18.0	17.2	16.4	15.8	15.1				

The results show that a much lower skin thickness of as little as 3mm for the edgewise laminations can be used whilst still maintaining sufficient shear strength. The use of the 24mm top and bottom skin now carries enough of the tensile stress so that the core material is below its maximum of 5.97 MPa.

This orientation of skin and core material provides another possibility for usage as transom decking and will be further investigated in chapter 5. Finite Element model for the beams with 4 laminations

is presented in Chapter 6. 4 laminates was chosen as it was the most laminates possible whilst still maintaining more core material than skin.

4.6. Conclusions

With the given loading for a train and the limited dimensions required of 290 w x 209 h, the laminated composite sandwiches requires significant amounts of skin material. It is not recommended to replace individual transom beams with laminated composite sandwiches in either the flatwise or edgewise orientation. For the combination arrangement however there is potential for replacement which should be further investigated, but which is beyond the scope of this project.

Chapter 5 - Transom Panel

5. Rail Loads for Bridge Deck Panel

The proposed dimensions (mm) of 2500(L) x 1200(W) x 209(H) is proposed for the panel. This allows rail attachments at 600mm centres whilst still allowing 300mm at either end of the panel as shown below in Figure 16. These dimensions also represent those the manufacturer makes the panels in.

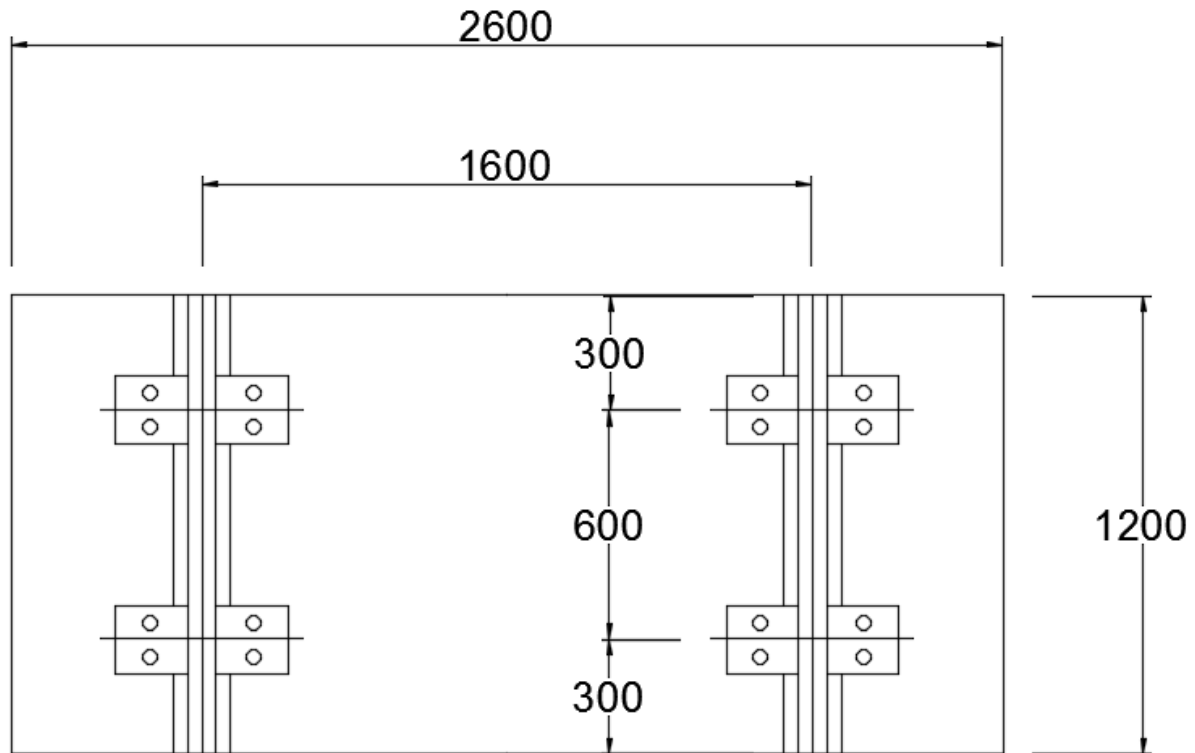


Figure 16: Proposed Panel Layout

The dimensions of the rail were sourced from the (Onesteel, 2011) rail track material catalogue for 68 Kg rail. The width of the bottom flange is 152.4 mm. For ease of modelling, the width has been set to 100mm.

From Chapter 3 it was shown that according to AS5100 the rail load is distributed over 1.2 metres of rail. Accordingly the 1.2 metre wide panel carries the full load of $\frac{1}{2}$ of an axle load of 360kN. The rail load is therefore 180 kN / 1.2 m which equals 150 kN/m.

The new factored load is now $(1+\alpha) \cdot \text{Load Factor} \cdot \text{Load}$

Where α is still 1.6, and the load factor is also 1.6.

This now makes the load $2.6 \cdot 1.6 \cdot 150 = 624$ kN/m

The bending moment for the panel is now $624 \cdot 1.2 \cdot 0.25 = 187.2$ kN.m

The shear is $(\frac{2}{3} \cdot 1.6) \cdot 1.6 \cdot 180 = 595.2$ Kn

5.1. Analysis in bending/Shear

Theoretical exploration of the stress in the core and skin for flatwise, edgewise and combination orientation is performed to determine the best candidate for potential use as rail bridge transom decking in bending.

5.1.1. Multiple Flat Sandwiches

The results for the panel with up to 11 laminations are shown below in Table 12. The maximum number of laminations was set at 11 due to the overall dimension of the individual sandwich layers being around 20mm which is desirable as it is the most easily produced in the factory. Adjustment of the excel spreadsheet developed earlier is used to produce the results as it allowed for easy adjustment of panel width, depth, skin thickness and number of laminations.

Table 12: Multiple Flatwise Layout Panel

Laminations	2	3	4	5	6	7	8	9	10	11
Overall Dim	104.5	69.67	52.25	41.80	34.83	29.86	26.13	23.22	20.90	19.00
Skin Thickness	10	9	7	6	5	5	4	4	3	3
Core Thickness	84.5	51.7	38.3	29.8	24.8	19.9	18.1	15.2	14.9	13.0
Overall height	209	209	209	209	209	209	209	209	209	209
EI Panel ($\times 10^{12}$)	3.96	4.31	4.25	4.37	4.33	4.78	4.49	4.86	4.26	4.55
Stress outer skin (Mpa)	63.40	58.14	59.04	57.35	57.95	52.44	55.91	51.55	58.84	55.09
Stress most extreme core Tensile (Mpa)	5.95	5.51	5.72	5.61	5.72	5.18	5.58	5.14	5.93	5.55
Shear (Core) (Mpa)	1.19	1.02	0.99	0.95	0.95	0.87	0.92	0.85	0.95	0.90
Max Shear Beam	2247	2638	2694	2806	2806	3085	2918	3141	2806	2974

5.1.2. Multiple Edge Sandwiches

Results for the panel with up to 12 laminations are shown below in Table 13.

Table 13: Edgewise Multiple Sandwich Layout panel

Laminations	2	3	4	5	6	7	8	9	10	11	12
Overall Dim	600	400	300	240	200	171	150	133	120	109	100
Skin Thickness	90	70	50	40	30	26	23	20	18	17	15
Core Thickness	420	260	200	160	140	119	104	93.3	84.0	75.1	70
Overall Width	1200	1200	1200	1200	1200	1200	1200	1200	1200	1200	1200
EI ($\times 10^{12}$)	4.36	4.88	4.71	4.71	4.36	4.39	4.43	4.36	4.36	4.48	4.36
Stress skin Top/Bot (Mpa)	57.5	51.3	53.2	53.2	57.5	57.0	56.6	57.5	57.5	55.9	57.5
Stress core top/bot (Mpa)	5.97	5.33	5.52	5.52	5.97	5.92	5.87	5.97	5.97	5.80	5.97
Shear Skin (Mpa)	5.74	5.21	5.38	5.38	5.74	5.70	5.67	5.74	5.74	5.61	5.74
Beam Max Shear (kN)	2881	3173	3076	3076	2881	2901	2920	2881	2881	2949	2881

5.1.3. Multiple Combination Panel

The results for the panel with 10 to 20 edge laminations are shown below in Table 14. The required amount of laminations for a panel which comprised 20mm individual laminations is 60, which was determined to be unfeasible to manufacture.

Table 14: Combination Layout Panel

Laminations	10	11	12	13	14	15	16	17	18	19	20
Lamination Skin Thickness	3	3	3	3	3	3	3	3	3	3	3
Core Thickness	114	103.1	94.0	86.3	79.7	74.0	69.0	64.6	60.7	57.2	54.0
Overall Width	120	109	100	92	86	80	75	71	67	63	60
Top/Bottom Skin Thickness	10	10	10	10	10	10	10	10	10	10	10
EI Total ($\times 10^{12}$)	4.33	4.37	4.41	4.45	4.49	4.53	4.57	4.61	4.64	4.68	4.72
Stress skin top/bot (Mpa)	57.8	57.35	56.8	56.3	55.8	55.3	54.9	54.4	53.9	53.5	53.1
Stress core top/bot (Mpa)	5.43	5.38	5.33	5.29	5.24	5.20	5.15	5.11	5.07	5.02	4.98
Shear Stress Skin (Mpa)	12.8	12.62	12.3	12.1	11.9	11.6	11.4	11.2	11.0	10.8	10.6

5.2. Analysis in Shear

Theoretical analysis of the shear in the core for flatwise and shear in the skin for edgewise and combination orientations is performed to predict the best suitable candidate for potential use as rail bridge transom decking in shear. The results are shown in Table 12 for the core in flatwise, Table 13 for the skin in edgewise and Table 14 for the skin in edgewise for combination layout.

5.3. Conclusions

It is interesting from the results of Table 12 and Table 13 that the flexural stiffness is similar when the panels reach around 10 laminations. The skin thickness for the sandwich in the flatwise layout being 20.9 mm has the advantage of being easier to create due to the production process being set up for individual panels of around 20mm thickness. Also when the beam reaches around 10 laminations the beam maximum shear is similar at around 2800 Kn.

The combination layout shows promise with a similar flexural stiffness of 4.3×10^{12} Nmm² and with only an edgewise skin thickness of 3mm. The overall individual panel width of around 70mm or more will cause production difficulty as the width is much more than the usual 20mm. The 10 mm thick top and bottom skin will increase the complexity of the design with another 2 layers of skin required to be bonded to the edges of the laminations that have already been bonded together. Due to the simplicity of existing manufacture, the obvious choice to progress with is the panel with 10 layers of 20mm sandwiches in a flatwise layout.

Chapter 6 - Finite Element Analysis

6. Finite Element Analysis

Beams and panels are modelled using the Strand7 Finite element analysis program. Skins and the core are made from Hexa16 bricks and the beam is subdivided once the model has been created. Table 15 summarizes the number of bricks, nodes and the computation time. The naming convention is organised with the letter B for Beam, P for Panel, S and M representing a single or multiple layer sandwich respectively, a digit representing the number of layers, with the flatwise or edgewise designated F or E respectively. The computer used to model the beam is a high performance 64 bit ASUS gaming laptop with Core i7 processor at 2.4 Ghz and 16 GB memory. This level of computing power enables the specimens to be analysed as a whole. The rail track is added to the beam at the 250 mm offset centre line, represented by a 100mm wide plate and 30mm thick. The point load was transformed into a normal pressure in order to distribute the load evenly over the plate. The corresponding pressure is $374.4 \times 10^3 / (100 \times 290) = 12.91$ Mpa for the 290 x 209 mm beam. The panel load was previously determined as 624 Kn/m with the panel being 1.2 metres wide this equals 748.8 kN. The pressure is therefore $(748800 / 100 \times 1200) = 6.24$ Mpa

Table 15: F.E. model for Sandwich Beam

Specimen	Number Bricks	Number Nodes	CPU Time
BS1F	181440	193851	2 Hrs 42 Mins 32 Sec
BM4F	233856	250154	2 Hrs 15 Mins
BM4E	60480	71475	6 Mins 47 Sec
BM4C	133056	174913	5 min 24 Sec
PM10F	201600	215475	2 Hrs 18 Mins 43 sec
PM10E	168000	208974	13 Mins
PM10C	238560	273445	2 Hrs 21 Mins 54 sec

6.1. Finite Element Models

The models are presented below before solving to give an idea of the layout of the sandwich. The core is red and the skins are blue. The force is represented by the brown arrows and the edges of the beam are supported by nodes with x,y,z limited movement and only rotation about the Y axis allowed. The model was run with linear static solver.

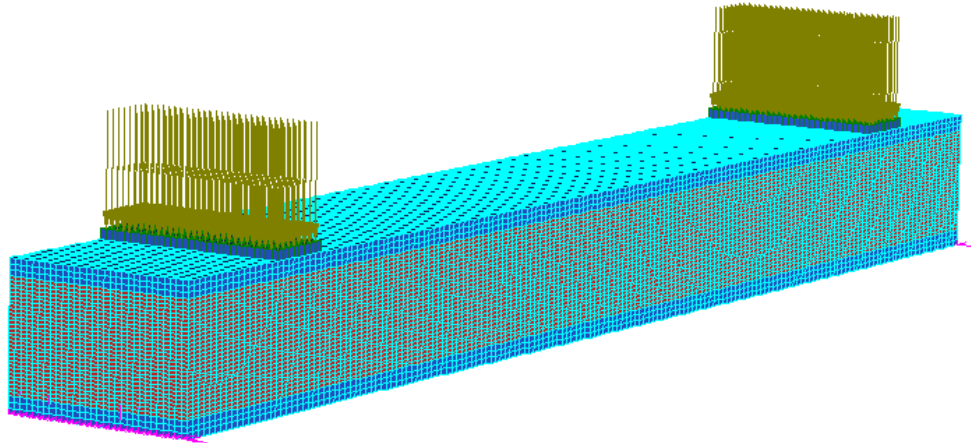


Figure 17: F.E. Model for specimen BS1F

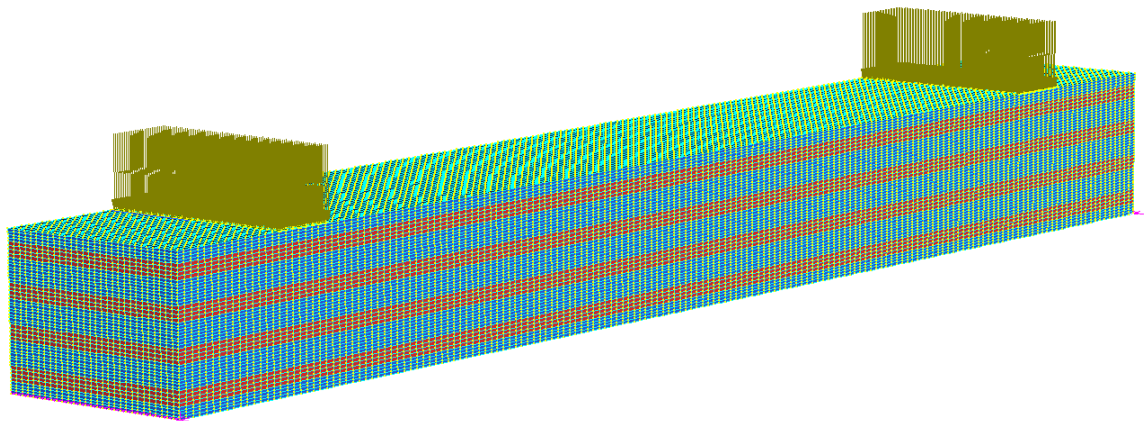


Figure 18: F.E. Model for Specimen BM4F

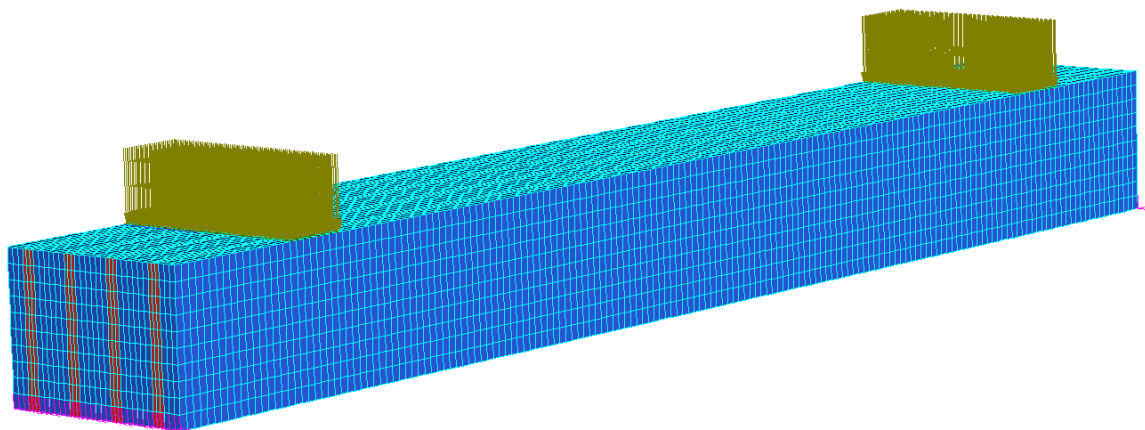


Figure 19: F.E. Model for Specimen BM4E

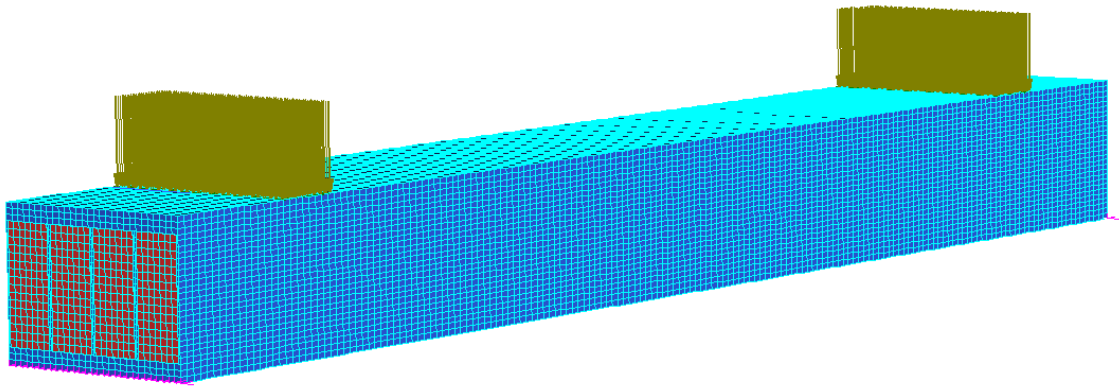


Figure 20: F.E. Model for Specimen BM4C

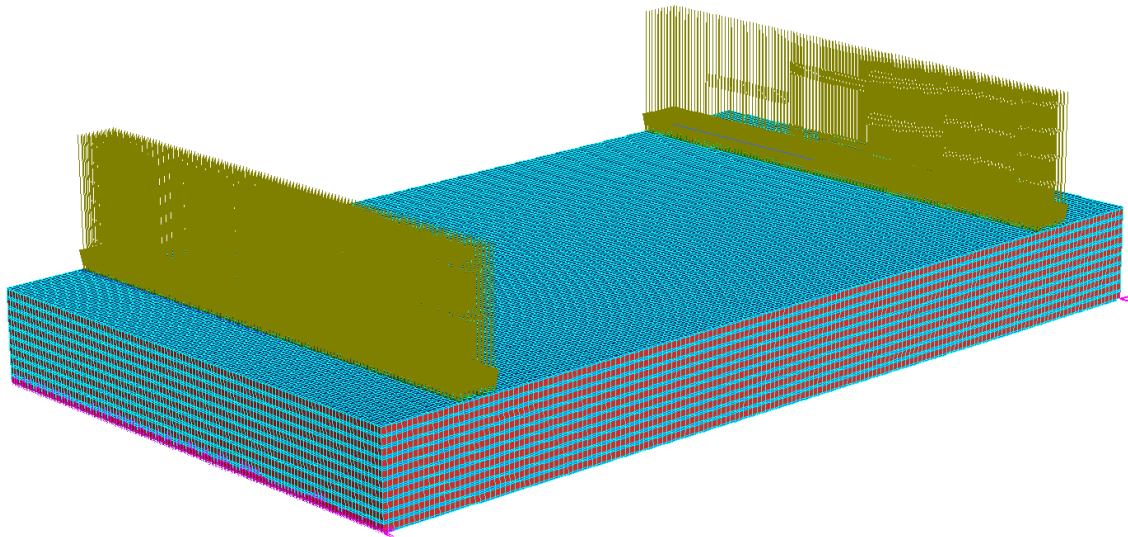


Figure 21: F.E. Model for Specimen PM10F

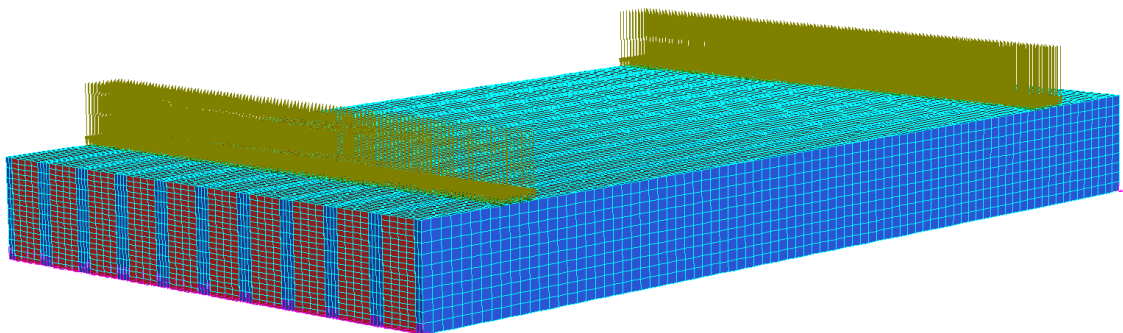


Figure 22: F.E. Model for Specimen PM10E

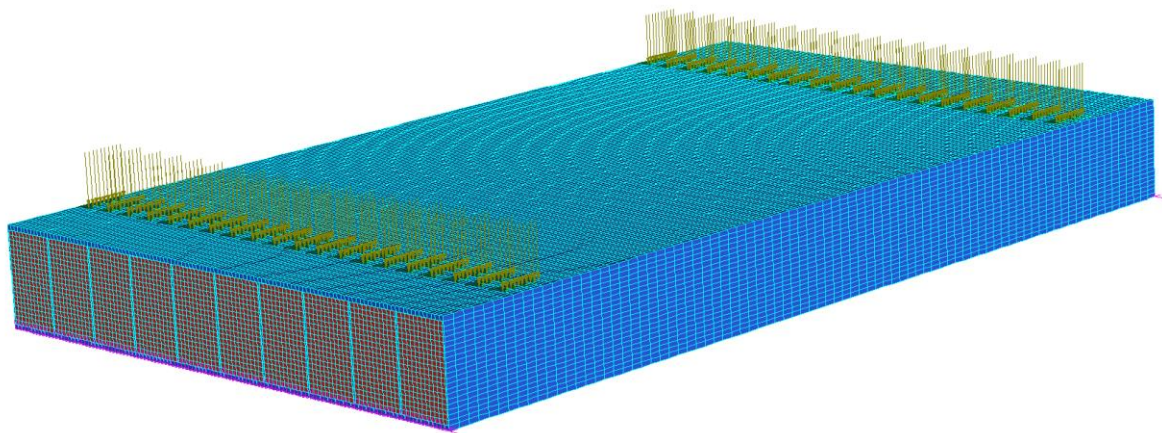


Figure 23: F.E. Model for specimen PM10C

6.2. Modelling Results

6.2.1. Transom Beams 290 w x 209 h

The following section presents results of finite element modelling for beams that were aimed to mimic the dimensions of existing transoms.

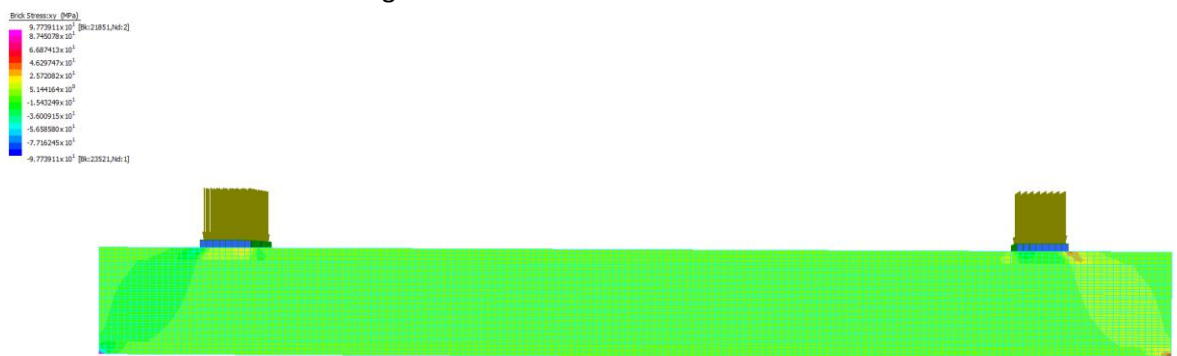


Figure 24: F.E. Model BS1F Shear

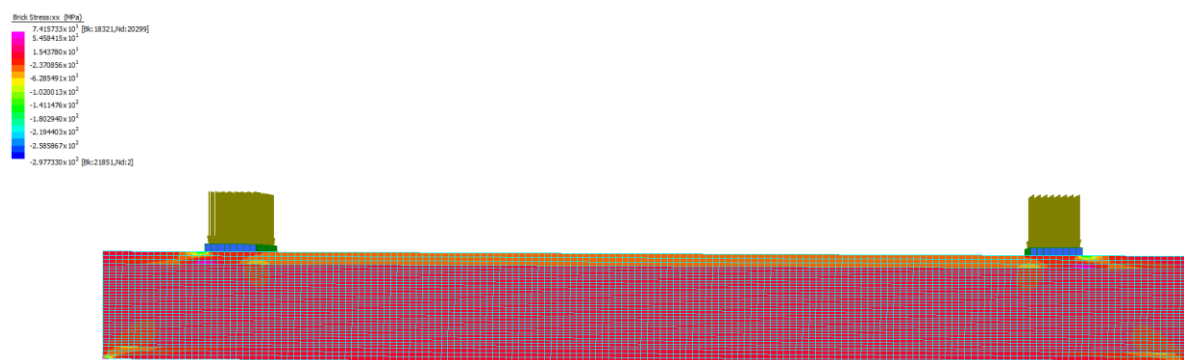


Figure 25: F.E. Model BS1F Stress

The maximum stress is concentrated around the node restraints and rails which is not accounted for with the numerical analysis. The shear in the skins in areas other than the loading and restraint points is less than their maximum of 27.8 Mpa. The maximum core tensile stress according to the model is 8.8 Mpa, again, at the location of the nodal restraint. The values otherwise are less than the core maximum tensile stress of 5.97 Mpa. The beam would seem appropriate for the task.

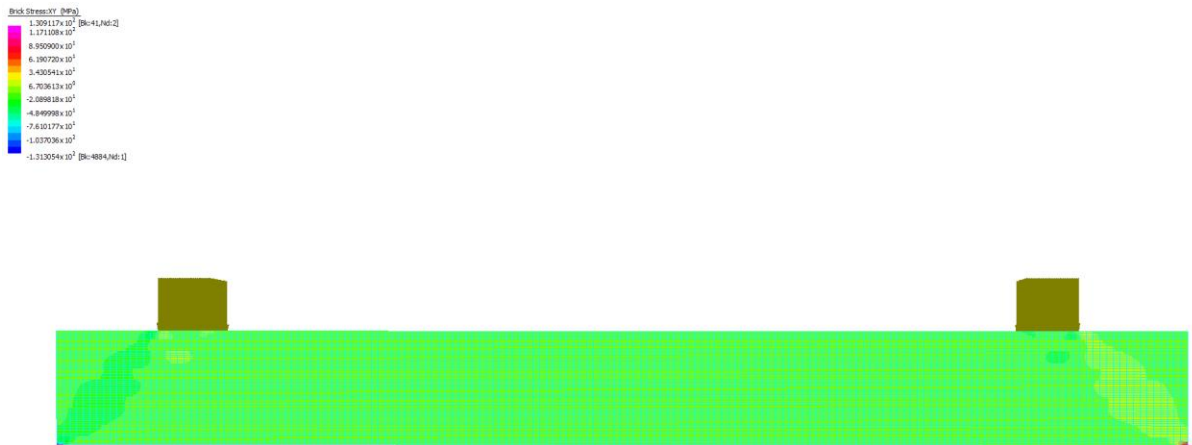


Figure 26: F.E. Model BM4F Shear

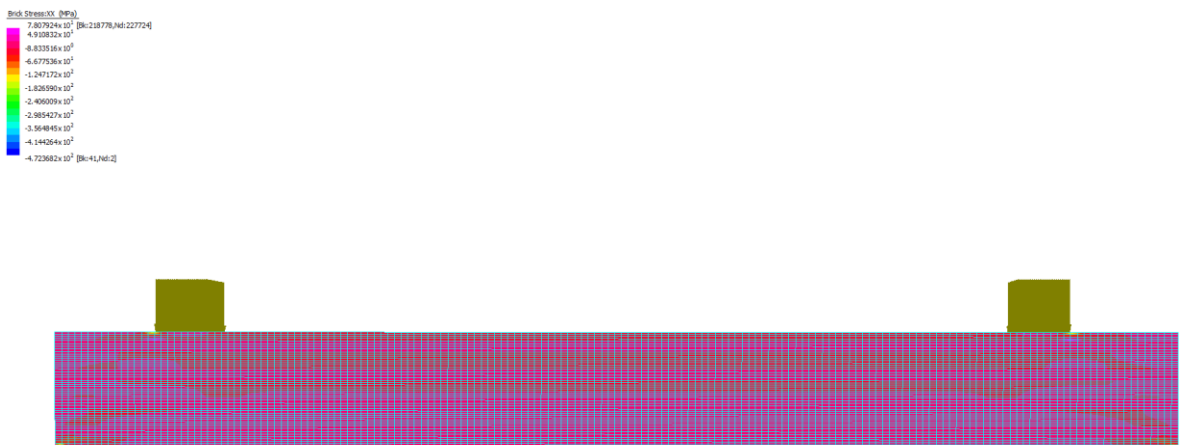


Figure 27: F.E.M. BM4F Axial Stress

Again for specimen BM4F the maximum axial stresses are around the nodal restraints and rail edges. The beam otherwise develops less stress and shear than the maximums for the skin and core.

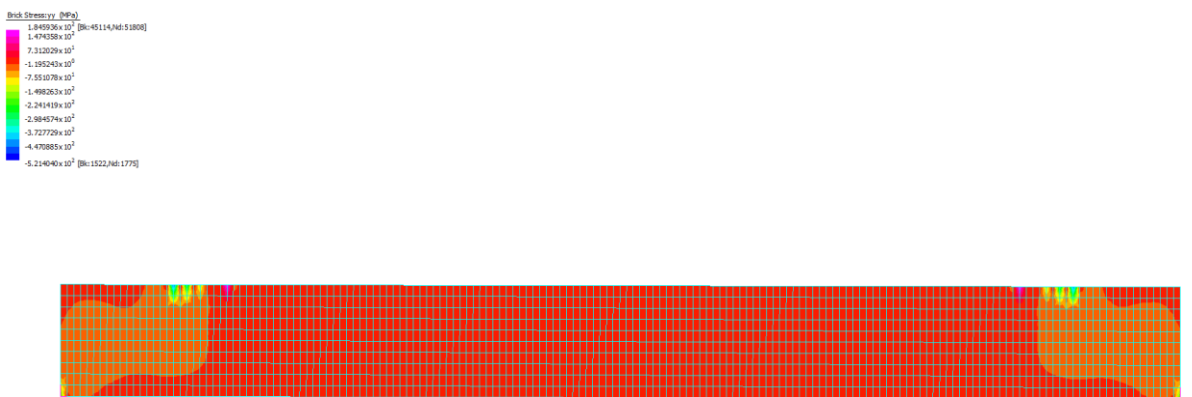


Figure 28: F.E. Model BM4E Shear

Chapter 6 - Finite Element Analysis

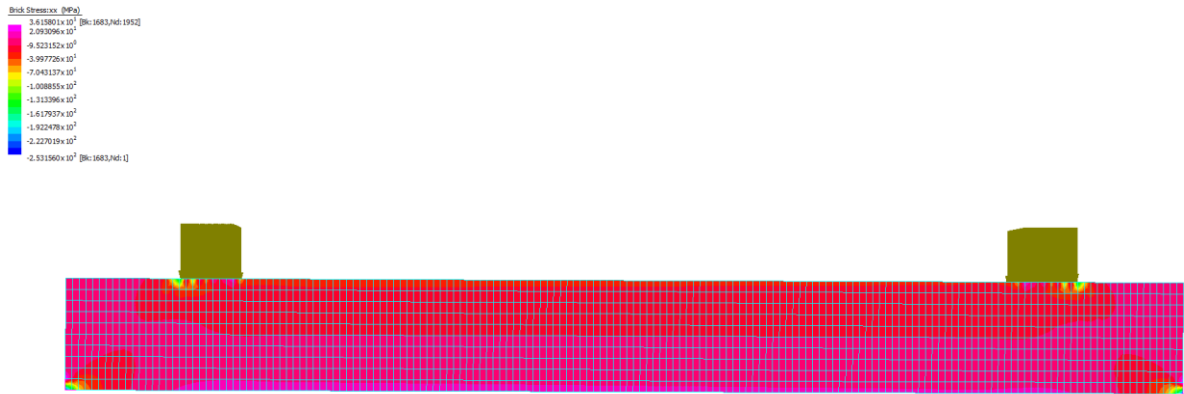


Figure 29: F.E. Model BM4E Axial Stress

The results for BM4E show that the beam is generally sufficient, with the skins having less than 27.8 Mpa shear in the skin. The axial force is again generally sufficient except for around the rail and nodal restraints.

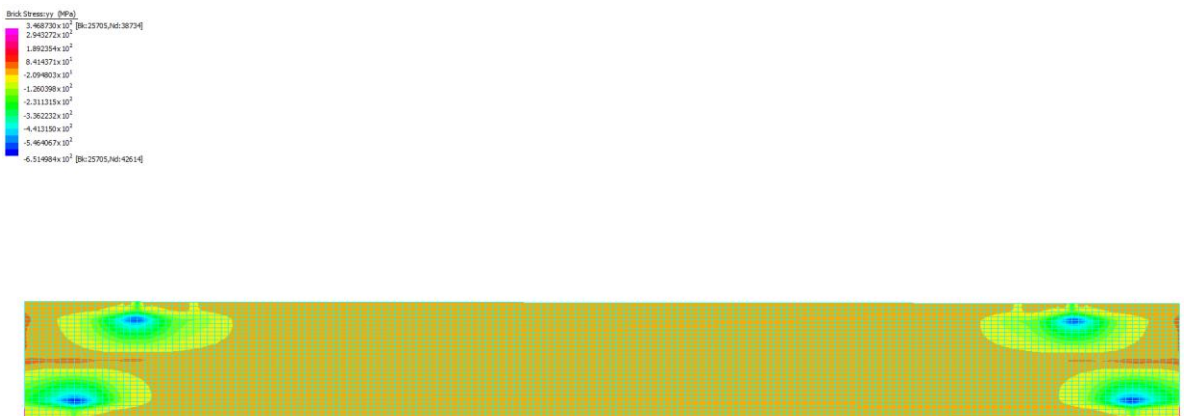


Figure 30: F.E. Model BM4C Shear

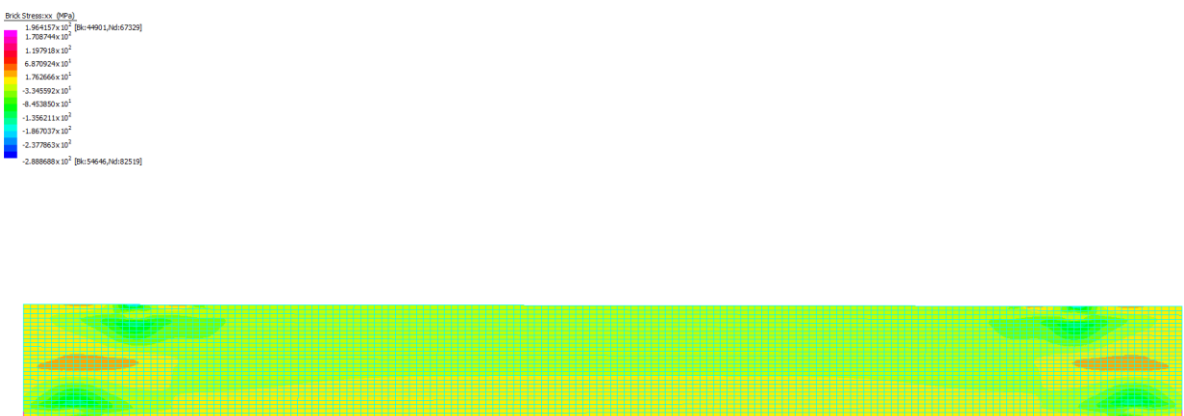


Figure 31: F.E. Model BM4C Axial Stress

The combination beam shows the most promise with the limited dimensions available when arranged as a bridge transom beam. It shows reduced stress around the loading points, possibly due to thicker skin material at these points; there are some rather high shear within the beam edge skins

that may cause localised failure. This may be remedied by increasing the thickness of the skin on the edges of the beam.

6.2.2. Panels 1200 w x 209 h

The following section presents the finite element model results for the panel arrangements.

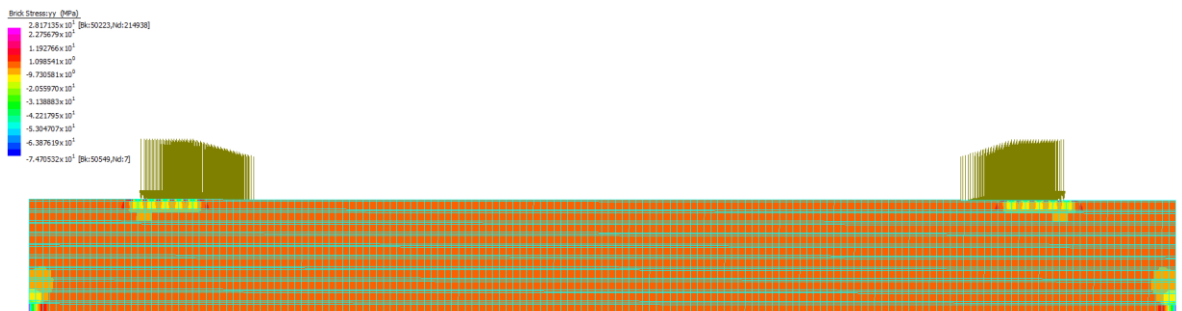


Figure 32: F.E. Model PM10F Shear

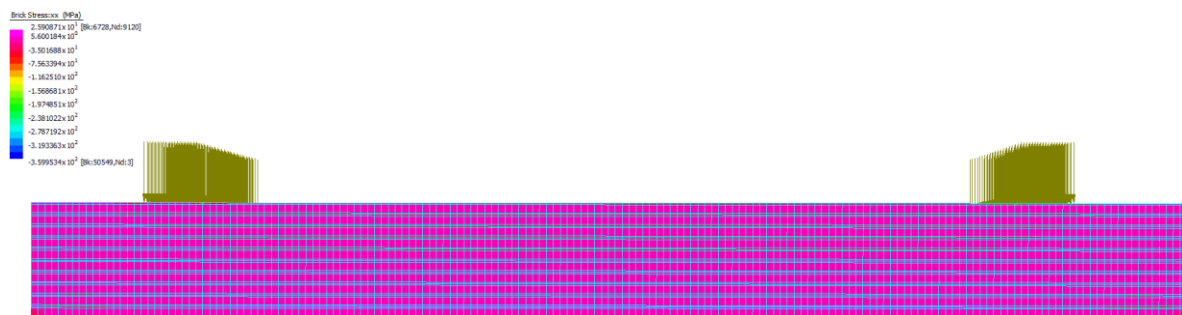


Figure 33: F.E. Model PM10F Axial Stress

It is clear that when the laminations are created wider into a panel of 1200 mm width the stress is dramatically reduced. The stress for the flatwise panel layout is predominantly compressive. The concentrations around the nodal restraints and rail may be reduced further through the use of thicker skin at the top under the rails as shown in specimen BM4C and applied also to the bottom of the panel. Deflections at mid span are listed at 11.3 mm.

Chapter 6 - Finite Element Analysis

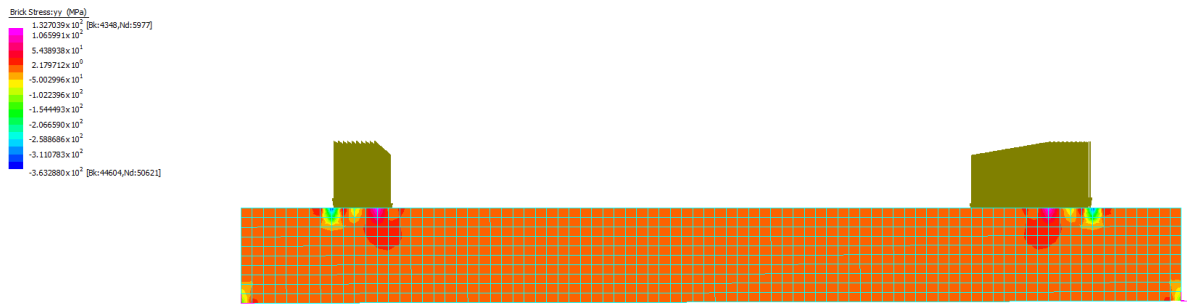


Figure 34: F.E. Model PM10E Shear

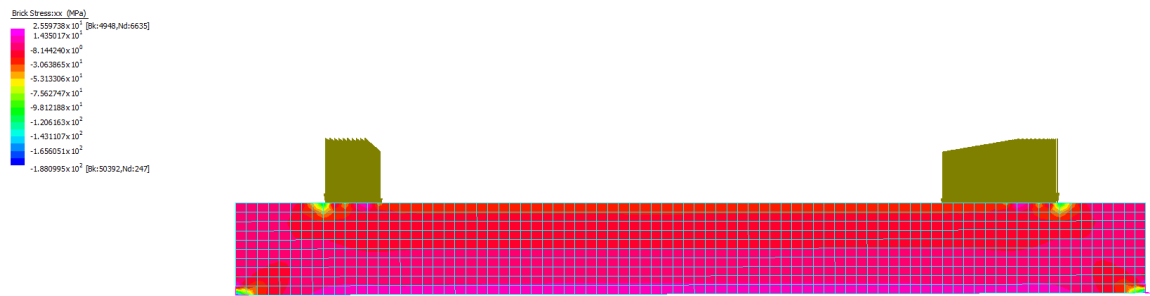


Figure 35: F.E. Model PM10E Axial Stress

The edgewise layout shows that the stresses are a mix of compressive and tensile. The deflection at mid span is now listed as 6.5 mm which indicates the beam has a higher flexural stiffness as expected from the numerical calculations, predominantly due to the thickness of the skin in the edgewise direction providing increased stiffness.

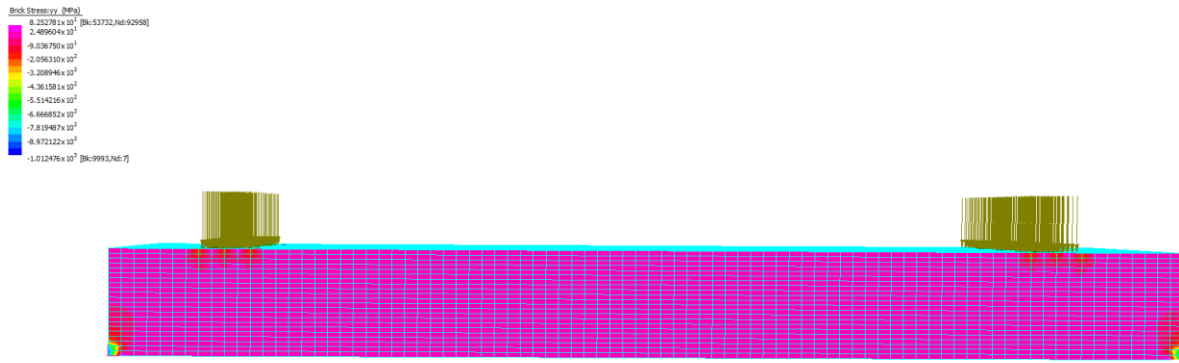


Figure 36: F.E. Model PM10C Shear

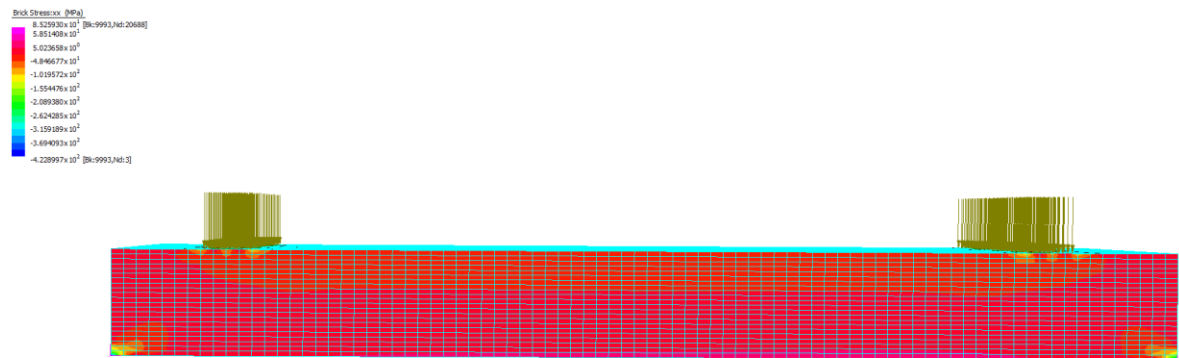


Figure 37: F.E. Model PM10C Axial Stress

Displacement for the Combination panel is 12.5 mm, showing a similar flexural stiffness to the flatwise layout panel. The reduction in stiffness is mainly due to the very thin 3mm skins used to produce the edgewise layout panels. As previously mentioned the thicker 10mm skins at the top and bottom has helped reduce the stress points about the node restraints and the rail.

Chapter 7 - Conclusions

7. Conclusions

7.1. Summary

A new type of rail bridge transom involving the use of decking panels has been introduced to improve safety of railway bridges. Current available materials do not meet the criteria for use as decking panels without having trade-offs in terms of durability, life span or characteristic material properties. The development of fibre composite technologies that can mimic the desirable properties of wood without the accompanied drawbacks of durability and limited life has enabled them to become a viable alternative.

The literature investigation conducted suggests that the fibre composite sandwich can be produced that mimics the properties of hardwood, and are almost maintenance free along with being fire resistant. This project is the first to examine a laminated composite sandwich panel constructed from the unique fibre composite sandwich panel for use as rail bridge decking.

7.2. Major Conclusions

A study has been undertaken on various combinations of skin and core thicknesses of a unique fibre composite sandwich in a variety of layouts. The following represents the major findings of this study:

- Laminating the composite sandwiches together into a layered panel, results in a more stable section than for an individual sandwich in terms of flexural stiffness.
- The greater the skin thickness for layer laminations, the greater was the flexural stiffness of the panel.
- In the flatwise layout the increasing ratio of skin to core with increasing laminations resulted in an increase in shear capacity.
- The flexural stiffness of beams created in an edgewise layout is increased to that of a flatwise layout for equal skin amounts, which is an advantage due to the lower deflections for stiffer beams giving better serviceability.
- The shear capacity of panels with an edgewise layout is increased to those of flatwise layout, however, there is significant complexities of the panel construction in both the edgewise and combination layout; any reduction in shear stress should be considered against this increased production complexity.
- With limited dimensions of width or height or both, the edgewise layout requires the same total thickness of skin and core no matter how many laminations are used.
- Creating another layer of skin onto the edgewise layout panel provides additional bending capacity but increases the complexity of construction.

7.3. Application to railway transom decking

From the theoretical and finite element analysis of laminated composite sandwich panels it appears that all the designs listed will cope with the static loads expected for a railway bridge, the implementation comes down to the designs practicality for production. The most obvious candidate for production is the laminated flatwise panel with 10 laminations of around 20mm height which is

ideal considering the manufacturers ability to mass produce individual sandwich panels in these dimensions.

7.4. Future recommended research

It is recommended that full scale laboratory load testing should be performed on multiple layer sandwiches of 1200 mm wide 2400 metre long, 20 mm thick sandwich panels stacked 10 high to form an overall thickness (including glue lines) of 209 mm in order to confirm the strength of the panel.

Stress cycling needs to be performed on the panel in order to determine the reaction over time to the expected repeated loads to provide an estimate of durability.

The ability of the panel to effectively hold rail fastenings without movement or error should be investigated.

Where dimensions for height and width are limited, the combination orientation of edgewise laminations with an additional top and bottom skin showed promise. There is an opportunity for further analysis of the combination arrangement for application as structural members due to the increase in flexural stiffness and shear capacity.

Finally, a thorough cost/benefit analysis should be undertaken which takes into consideration the total lifetime cost of the fibre composite panel compared with existing transoms. The cost for fibre composite panels should decrease as production becomes more automated which should also be taken into consideration.

References

Adams, J 1991, *Cost Effective Strategy for Track Stability and Extended Asset Life through Planned Timber Sleeper Retention*, Institution of Engineers, Australia, Barton, ACT.

Akbiyik, A, Lamanna, AJ & Hale, WM 2007, 'Feasibility investigation of the shear repair of timber stringers with horizontal splits', *Construction and Building Materials*, vol. 21, no. 5, pp. 991-1000, <<http://www.sciencedirect.com/science/article/pii/S0950061806000390>>.

B4B, 2011, Boral for Builders, Boral National Publication, online, [http://www.boral.com.au/brochures/ordering/PDF/BBP_05402B4B_News_LR%20\(3\).pdf?pdfName=BBP_05402B4B_News_LR%20\(3\).pdf](http://www.boral.com.au/brochures/ordering/PDF/BBP_05402B4B_News_LR%20(3).pdf?pdfName=BBP_05402B4B_News_LR%20(3).pdf)

Bekuit, J.R.B., Oguamanam, D.C.D. and Damisa, O. (2007). A quasi-2D finite element formulation for the analysis of sandwich beams. *Finite Elements in Analysis and Design*, 43, 1099-1107.

Bolin, CA, Christopher, AB & Stephen, TS 2013, 'Life Cycle Assessment of Creosote-Treated Wooden Railroad Crossties in the US with Comparisons to Concrete and Plastic Composite Railroad Crossties', *Journal of transportation technologies*, vol. 3, no. 2, pp. 149-61.

Duan, L, Chen, W. F. 1999, *Bridge engineering handbook*, CRC Press, Boca Raton FL.

Esveld, C 2001, *Modern railway track*, 2nd ed. edn, MRT Productions, The Netherlands.

Ferdous, W & Manalo, A 2014, 'Failures of mainline railway sleepers and suggested remedies – Review of current practice', *Engineering Failure Analysis*, vol. 44, pp. 17-35, <<http://www.sciencedirect.com/science/article/pii/S1350630714001344>>.

Garlock, M, Paya-Zaforteza, I, Kodur, V & Gu, L 2012, 'Fire hazard in bridges: Review, assessment and repair strategies', *Engineering Structures*, vol. 35, pp. 89-98, <<http://www.sciencedirect.com/science/article/pii/S0141029611004408>>.

Griffin, DWP, Mirza, O, Kwok, K & Kaewunruen, S 2014, 'Composite slabs for railway construction and maintenance: a mechanistic review', *The IES Journal Part A: Civil & Structural Engineering*, vol. 7, no. 4, pp. 243-62, viewed 2015/08/13, <<http://www.tandfonline.com/doi/abs/10.1080/19373260.2014.947909>>.

Hay, WW 1982, *Railroad engineering*, 2nd ed. edn, Wiley, New York.

Ikarashi, Y, Kaniwa, M-a & Tsuchiya, T 2005, 'Monitoring of polycyclic aromatic hydrocarbons and water-extractable phenols in creosotes and creosote-treated woods made and procurable in Japan', *Chemosphere*, vol. 60, no. 9, pp. 1279-87, <<http://www.sciencedirect.com/science/article/pii/S0045653505001955>>.

Ivanoff, V 1995, *Engineering Mechanics: An Introduction to Statics, Dynamics and Strength of Materials*, McGraw-Hill.

Loccomposites, Product Brochure, [ONLINE] Available at: <http://www.icsservices.com.au/wkg/pdfs/Carbonlocmanualgeneral5.pdf>. <Viewed 10th February 2015.

Manalo, Allan (2011) Behaviour of fibre composite sandwich structures: a case study on railway sleeper application. [Thesis (PhD/Research)] (Unpublished)

Manalo, AC, Aravinthan, T & Karunasena, W 2010, 'Flexural behaviour of glue-laminated fibre composite sandwich beams', *Composite Structures*, vol. 92, no. 11, pp. 2703-11, <<http://www.sciencedirect.com/science/article/pii/S0263822310000966>>.

MCKAY, GVEM 2013, 'Recent Australian Developments in Fibre Composite Railway Sleepers', *Electronic Journal of Structural Engineering*, vol. 13, no. 1, pp. 62-6.

Monrroy, M, Ortega, I, Ramírez, M, Baeza, J & Freer, J 2011, 'Structural change in wood by brown rot fungi and effect on enzymatic hydrolysis', *Enzyme and Microbial Technology*, vol. 49, no. 5, pp. 472-7, <<http://www.sciencedirect.com/science/article/pii/S0141022911001864>>.

P. A. Mendis, 2013, A Review of Behaviour of Prestressed Concrete Sleepers, Special Issue: Electronic Journal of Structural Engineering 13(1).

Poisson, F & Margiocchi, F 2006, 'The use of dynamic dampers on the rail to reduce the noise of steel railway bridges', *Journal of Sound and Vibration*, vol. 293, no. 3–5, pp. 944-52, <<http://www.sciencedirect.com/science/article/pii/S0022460X05008047>>.

Profillidis, VA 1995, *Railway engineering*, Avebury Technical, Aldershot.

Railcorp, 2015, New underbridges, track structure requirements, drainage and waterproofing and derailment containment devices, Technical Note, Transport for NSW, Online, <<http://www.asa.transport.nsw.gov.au/sites/default/files/asa/railcorp-legacy/disciplines/civil/esc-310.pdf>>

StandardsAustralia 2004, 'Australian Standard® Bridge design'.

Ticoalu, A, Aravinthan, T & Karunasena, W 2008, 'An investigation on the stiffness of timber sleepers for the design of fibre composite sleepers', in *20th Australasian Conference on the Mechanics of Structures and Materials (ACMSM 20): Futures in Mechanics of Structures and Materials: proceedings of the 20th Australasian Conference on the Mechanics of Structures and Materials (ACMSM 20): Futures in Mechanics of Structures and Materials*, T Aravinthan, et al. (eds.), Taylor & Francis (CRC Press), Toowoomba, Australia, pp. 865-70.

Van den Bulcke, J, De Windt, I, Defoirdt, N, De Smet, J & Van Acker, J 2011, 'Moisture dynamics and fungal susceptibility of plywood', *International Biodeterioration & Biodegradation*, vol. 65, no. 5, pp. 708-16, <<http://www.sciencedirect.com/science/article/pii/S0964830511000710>> <<http://www.ncbi.nlm.nih.gov/pmc/articles/PMC3993986/pdf/nihms562096.pdf>>.

Vinden, P, Torgovnikov, G & Hann, J 2011, 'Microwave modification of Radiata pine railway sleepers for preservative treatment', *European Journal of Wood and Wood Products*, vol. 69, no. 2, pp. 271-9, <<http://dx.doi.org/10.1007/s00107-010-0428-8>> <<http://link.springer.com/article/10.1007%2Fs00107-010-0428-8>>.

Webb, DA 2005, 'Tie Guide', *Handbook for Commercial Timbers used by the crosstie industry*.

References

W.Y. Yun, L. Ferreira Prediction of the demand of the railway sleepers: a simulation model for the replacement strategies *Int J Prod Econ*, 81–82 (2003), pp. 589–595 T. Ngo J. Taherinezhad , M. Sofi &

Xu, G & Goodell, B 2001, 'Mechanisms of wood degradation by brown-rot fungi: chelator-mediated cellulose degradation and binding of iron by cellulose', *Journal of Biotechnology*, vol. 87, no. 1, pp. 43-57, <<http://www.sciencedirect.com/science/article/pii/S0168165600004302>>.

Yong, Yun Huang, The old Rail Bridge, Photograph, viewed 17th August 2015, <https://commons.wikimedia.org/wiki/File:The_old_rail_bridge.jpg>

Appendices

A. Flexural Stiffness flatwise and edgewise

For the sandwich having equal distance from the centroid of the beam to the centroid of both skin layers makes $d_i=d/2$

The equation for flexural stiffness is:

$$(EI) \quad A1$$

Where E = Young's Modulus of Elasticity, given in table 4.

I = Second moment of area

The equation for second moment of area about a given axis is :

$$I = \frac{bd^3}{12} + Ad_i^2 \quad A2$$

Where the moment of inertia for a rectangle is:

$$\frac{bd^3}{12} \quad A3$$

The transfer term for parallel axis area:

$$Ad_i^2 \quad A4$$

A= is the area

D_i= distance between axis

Combining equation A1 with equation A2 for the sandwich consisting of 1 core and 2 skins gives:

$$EI = E_c I_c + 2(E_s I_s)$$

$$\text{For the skins } I_s = \frac{bt^3}{12} + Ad_i^2$$

$$\text{but } d_i = \frac{d}{2}$$

$$\therefore I_s = \frac{bt^3}{12} + bt \left(\frac{d}{2}\right)^2$$

$$\text{making } EI = E_c \frac{bc^3}{12} + 2 \left[E_s \frac{bt^3}{12} + bt \left(\frac{d}{2}\right)^2 \right]$$

$$\therefore EI = E_c \frac{bc^3}{12} + E_s \left[\frac{bt^3}{6} + \left(bt \frac{d}{2} \right)^2 \right]$$